SIMULATION STUDY OF CENTRIFUGAL PUMP PERFORMANCE WITH VARIATION OF NUMBER OF BLADES

A Dissertation
Submitted in partial fulfillment of the requirements for the award of degree of

Master of Engineering

in

Thermal Engineering

Submitted by

PRASHANT KAUSHIK

(ROLL NO. 801283020)

Under the guidance of

MR. SATISH KUMAR
(ASSISTANT PROFESSOR)

MECHANICAL ENGINEERING DEPARTMENT

THAPAR UNIVERSITY, PATIALA-147004

JULY, 2014

CERTIFICATE

I here declare that the thesis entitled **"Simulation Study of Centrifugal Pump Performance With Variation of Number of Blades"** is an authentic record of my study carried out as requirements for the award of the degree of **Master of Engineering** in **Thermal Engineering** at **Thapar University**, **Patiala** under the supervision of **Mr. Satish Kumar**, Assistant Professor, Mechanical Engineering Department, Thapar University, Patiala during July 2012 to July 2014. The matter embodied in this report has not been submitted in partial or full to any other university or institute for the award of any degree.

Prashant kaushik

Date: 18/07/2014

Prashant Kaushik

(Roll No. - 801283020)

It is certified that the above statement made by the student is correct to the best of our knowledge and belief.

Mr. Satish Kumar

Mechanical Engineering Department

Thapar University, Patiala - 147004

Countersigned by

Dr. Ajay Batish

Professor & Head

Mechanical Engineering Department

Thapar University, Patiala – 147004

Dr. S.K. Mohapatra

Dean of Academic Affairs

Thapar University, Patiala – 147004

Dedicated to

My Parents

ACKNOWLEDGEMENTS

At first, my heartfelt thanks to the almighty for his abundant blessing showered on me throughout this Endeavour to complete the thesis work successfully. I have been persistently supported by my friends. I would like to record the support by my parents throughout my life. I would cherish every moment where my parents were so keen and curious to know about the details and progress of my work, particularly to my brother for the numerous discussions and his ever constructive advice. I express my deep sense of gratitude to them. The cooperation of all the elders of my family and relatives is also gratefully acknowledged.

My honorable guide **Mr. Satish Kumar**, Assistant Professor, Department of Mechanical Engineering, is a person to whom I shall always remain grateful for his excellent guidance, valuable discussions, encouragement, constructive criticism and his insights have strengthened this study significantly. He gave me a complete freedom to use my opinion, correcting whenever necessary in my dissertation.

I would like to thank our Head of the Department, **Dr. Ajay Batish**, who has been supportive at all times and accommodative.

Prashant Kaushik

Prashant Kaushik

ABSTRACT

The centrifugal pumps have been widely used for slurry transportation in thermal power plant, dredging, metallurgy, chemical industry, water conservancy, construction and environmental protection industries. Computational Fluid Dynamics (CFD) has become more popular approach for designing and performance evaluation of the complex machines. The FLUENT software with standard k-ε model is used to simulate the existing pump. Mixture model is used for simulate the two phase flow. Simulations of solid minerals suspension (coal, limestone and zinc tailings) are conducted at 1450 rpm and at different mass flow rate. Pump performance is computed by choosing the different diameter and volume fraction. The static pressure, volume fraction distribution at different concentration is analyzed. The particle diameter is varying. The simulation is conducted at 31μm and 175 μm particle diameter. It is found that the particle diameter has more effect on the volume fraction of coal. Pump performance is study with variation of number of blades at speed 1450 and 1750 rpm. The results show that that due to increase in the blade number and the rotational speed, the pump head increases.

Sr, No.	CONTENTS	Page. No

LIST OF FIGURES

LIST OF TABLES

Nomenclature

α_s	Volume concentration of solid in decimal point
α_k	Volume fraction of phase k (%)
C_{ws}	Solid concentration by weight
C_v	Volume fraction (%)
d	Particle diameter (m)
d_i	The average diameter of the two successive size of sieves
$\vec{F}$	Volume force (N)
f_i	Fraction of solid retained on a particular sieve
F_L	Limiting settling velocity factor
g	Gravitational acceleration (m/sec^2)
H	Total head (m)
η	The number of phase
$\frac{p_2}{pg}$	Delivery pressure gauge reading delivery side (m)
$\frac{p_1}{pg}$	Vaccum gauge reading at suction side (m)
P_{out}	Total pressure at volute outlet
P_{in}	Total pressure at impeller inlet
P_o	Power output (Kw)
p_k	Density of phase k (kg/m^3)
p_m	Density of the mixture (kg/m^3)
p_s	Density of the solid phase
p_l	Density of the carrier phase
p	Mass density of water (Kg/m^3)
Q	Flow rate (m^3/s)
S	Specific gravity of solid particle
S_L	Specific gravity of carrier phase
μ_l	Dynamic viscosity of the carrier phase

$\mu_{\boldsymbol{m}}$	Viscosity of the mixture (Pa.s)
$\vec{v}_{dr,k}$	Floating velocity of phase k (m/s)
$\vec{v}_{qp}$	Sliding velocity of phase k (m/s)
$\vec{v}_m$	Mass averaged velocity (m/s)
V_2	Velocity of fluid in delivery pipe (m/s)
V_1	Velocity of fluid in suction pipe (m/s)
W_{bs}	Weight of beaker and solid
W_b	Weight of beaker
W_{bw}	Weight of beaker and water
W_{bsw}	Weight of beaker, solid and water
Z_2	Delivery head (m)
Z_1	Suction lift (m)

CHAPTER 1

INTRODUCTION

A pump is a mechanical device that imparts energy to the fluids such as liquids and gases or sometimes slurries by mechanical action. It is a hydraulic machine, which convert mechanical energy into the hydraulic energy.

Pumps are classified as rotary, reciprocating or centrifugal. Gear, vanes, lobes are used by rotary pump to transfer fluid from inlet to outlet. Reciprocating Pumps are those which use pistons or diaphragms for giving the pressure to the fluid. In centrifugal pumps, fluid move by the action of centrifugal force which is imparted by rotating elements is called impeller which raises the kinetic and pressure energy of the fluid.

1.1 CENTRIFUGAL PUMP

Centrifugal pump is a device in which mechanical energy is converted into the pressure energy by means of centrifugal force acting on the fluid. Centrifugal pumps may be single or multi stage depending on the number of the impeller. At present time there are various types of centrifugal pump available in the market with single and double entry, with multiple rotor stages. Efficiency of the pump depends on the application. Centrifugal pump are used for many application and handle liquid and gases at relatively high pressure and temperature. Rotor and volute are the two main component of centrifugal pump. A centrifugal pump has two main components, a. The part which gives energy to the fluid generally known as impeller is called rotor and the part around which fluid moves is termed as casing. Efficiency of the centrifugal pump depends on the shape of the impeller. Structure of specific flow depends on the geometry of the pump. Recirculation and separation may occur at part flow conditions and due to the formation of the vapour bubbles, cavitations occur.

Due to the rotating impeller blade unsteadiness occurs in centrifugal pump which pass through the stationary volute cutwater and diffuser blade. Unsteady effects on the off design

condition and with respect to time, it effects the variation of mass flow through the centrifugal pump.

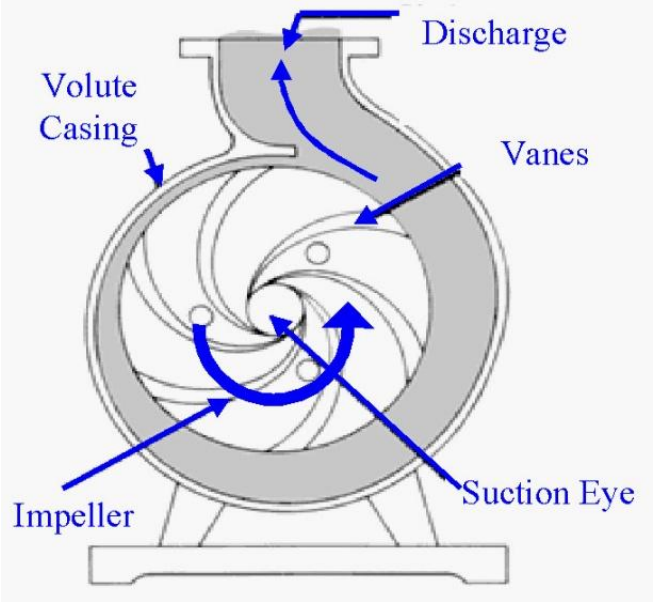

Figure 1.1: Centrifugal Pump [1]

Design of impeller and casing are very complex. To impart the energy efficiently to the fluid, the features of the impeller such a number of blades, inlet and outlet blade angle, leading and trailing edge, eye diameter must be considered carefully and specified. The volute of the pump may be circular or spiral and cross-sectional area must be circular, trapezoidal or rectangular shapes.

1.2 COMPONENTS OF CENTRIFUGAL PUMP

Centrifugal Pump consists the following main components:

1. Impeller

2. Casing

3. Suction Pipe

4. Delivery Pipe

1.2.1 Impeller

The impeller is mounted on a shaft coupled to driving unit which may be an electric motor or IC engine. It has the backward curved vanes which are mounted in series.

- **Open impeller**

  A front or a rear shroud is not present in open type of impellers. Such Pumps are used for handling mixture of water, sand, clay etc. It is made of generally made of forged steel.

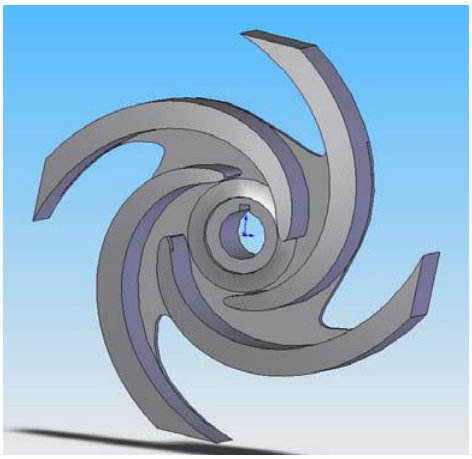

Figure 1.2: Open impeller [(2)]

- **Semi open impeller**

  In semi open impeller; there is only one shroud which presents either the front or the back of the impeller. It is used for viscous liquid such as sewage; paper pulp etc, choice of material for manufacturer of impeller is influenced by chemical nature of liquid to be handled.

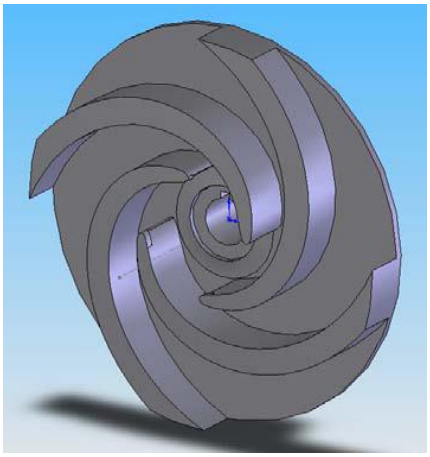

Figure 1.3: Semi-open impeller [2]

- **Shrouded or closed impeller**

  In this type of impeller, the vanes are covered with shrouds on both sides. It is used to handle non-viscous liquid such as ordinary water, hot water, hot oils and chemicals like acids etc.

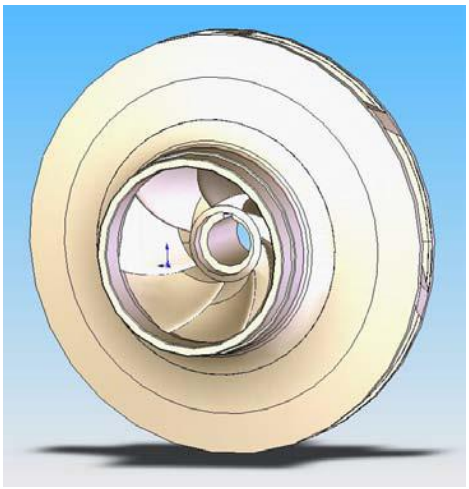

Figure 1.4: Closed impeller [2]

1.2.2 Casing

It is an airtight passage surrounding the impeller which consists suction and discharge arrangement. In this, the kinetic energy of water which is discharged at the impeller outlet is converted into the pressure energy before entering the delivery pipe.

- **Volute casing**

  It is a spiral type casing in which flow area gradually increases. Due to increase in the flow area velocity flow decreases. Due to eddies formation, large amount of energy is lost. In this type of casing, efficiency increases slightly.

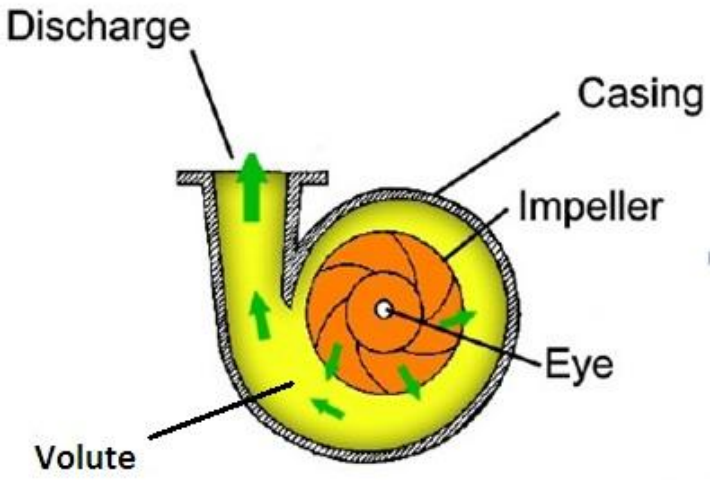

Figure 1.5: Volute casing [3]

- **Vortex casing**

  There is a little bit difference in volute casing and vortex casing. Vortex casing has a circular chamber between the impeller and casing. By presenting of this circular chamber, loss of energy due to eddies formation got reduce. So, It has the maximum efficiency than the volute casing.

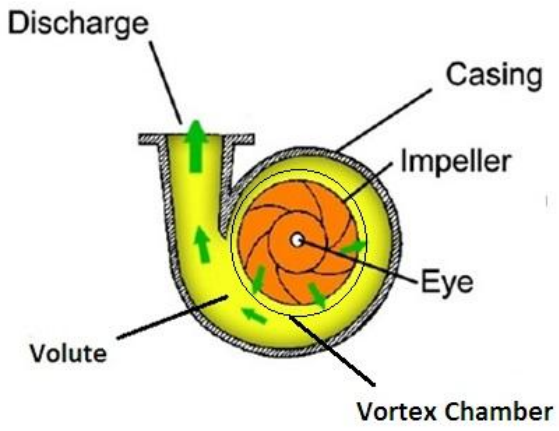

Figure 1.6: Vortex casing [3]

- **Diffuser casing**

  Diffuser casing has the series of the guide blade which is mounted on a ring. These guide vanes are designed such a manner that there is no shock when water comes from the impeller. To reduce the flow velocity, area of the guide vanes increases so that there is an increment in the water pressure.

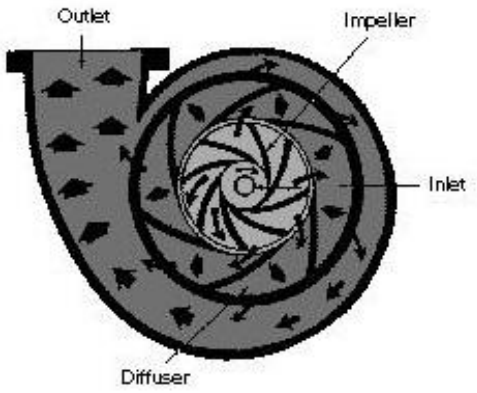

Figure 1.7: Diffuser casing [3]

1.2.3 Suction Pipe

It is a pipe which is connected to the pump inlet from one end while the other end of the pipe dips into water in a sump.

1.2.4 Delivery Pipe

It is a pipe which is connected to the pump outlet from one end while the other end of the pipe delivers waters at required height.

1.3 SLURRY

A mixture of solid and liquid is known as slurry. Slurry is classified into two types, settling slurry and non settling slurry.

Non-settling slurry

Non-Settling slurries necessitate the particles which are very fine and can form the stable homogeneous mixtures. These slurries act in a viscous manner but these have non-Newtonian characteristics.

Homogeneous mixture

The mixture in which solids are uniformly distributed is known homogeneous mixture.

Settling slurry

Coarser particles are used to form the settling slurries and tend to form an unstable heterogeneous mixture. These slurries are Heterogeneous types.

Heterogeneous mixture

The mixture in which solids are not uniformly distributed and tend to be more concentrated in the bottom of pipe is known homogeneous mixture.

1.3.1 Parameters of Slurry

The characteristics of slurry are determined by various factors like size of particles, solid concentration, turbulence in the flow field, viscosity of the liquid etc. The flow of slurry is different from a single phase fluid flow. For a single phase liquid with low viscosity, the

velocity of flow could be ranging from very low to high. Whereas, for slurry flow the velocity has to be more than critical velocity, otherwise, settling may occur in the slurry pipe line resulting blockage of flow passage.

Density of slurry

Density of slurry depends on density of solids, density of carrier phase and solid concentration in the mixture. The density of slurry (p_m) can be expressed as: (Baha, 2002)

$$p_m = \frac{100}{(C_{ws}/p_m)+(100-C_{ws})/p_l} \quad \text{..... (1.1)}$$

Where, C_{ws}= solid concentration by weight, p_m = density of the mixture

p_l = density of the carrier phase and p_s = density of the solid phase

The solid concentration by volume (C_v) can be determined as:

$$C_v = \frac{100C_{ws}/p_s}{(C_{ws}/p_s)+(100-C_{ws})/p_l} \quad \text{..... (1.2)}$$

Again, solid concentration by weight could be calculated as:

$$C_{ws} = \frac{C_v p_s}{C_v p_s+(100-C_v)} \quad \text{..... (1.3)}$$

Viscosity of slurry

The absolute or dynamic viscosity of slurry mixture depends on the concentration of the slurry. The relationship between dynamic viscosity and volume can be given by the following formula for different ranges of volume concentration.

(a) Slurry with Volume Concentration Less than 1% (Baha, 2002)

When volume concentration of solids is less than 1% in a solid-liquid mixture, then there is very less interactions present between the solid particles. In that case the relations between the dynamic viscosity and volume concentration could be expressed as:

$$\frac{\mu_m}{\mu_l} = 1 + 2.5\alpha_s \quad \text{..... (1.4)}$$

Where, α_s = volume concentration of solid in decimal point,

μ_m = dynamic viscosity of the slurry mixture

μ_l = dynamic viscosity of the carrier phase

(b) Slurry with Volume Concentration Less than 20 % (Baha, 2002)

When the solid concentration is high but less than 20%, then, dynamic viscosity can be expressed as

$$\frac{\mu_m}{\mu_l} = 1 + K_1\alpha_s + K_2\alpha_s^2 + K_3\alpha_s^3 + K_4\alpha_s^4 + \ldots \quad \text{..... (1.5)}$$

Where, $K_1K_2K_3K_4$ …….are constants

(c) Slurry with Very High Volume Concentration (Baha, 2002)

Thomas correlation could be use to determine the dynamic viscosity of solid-liquid mixture for very high volume concentration, as shown below:

$$\frac{\mu_m}{\mu_l} = 1 + K_1\alpha_s + K_2\alpha_s + Ae^{B\alpha_s} \quad \text{..... (1.6)}$$

Where, K_1=2.5, K_2=10.05, A=0.00273 and B=16.6

Critical velocity

Transportation of slurries consisting coarser particles in suspension could be done if the average velocity if more than a limiting value. This limiting velocity is called critical velocity. It can be calculated from Durand's formula: (Warman, 2009)

$$V_L = F_L\sqrt{2gD_P\frac{S-S_L}{S_L}} \quad \text{..... (1.7)}$$

Where D_P is inside diameter of pipe, S is specific gravity of solid particle, S_L is specific gravity of carrier phase and F_L is limiting settling velocity factor.

1.4 TRANSPORTATION OF SLURRY

A mixture of solid and liquid is known as slurry. Several methods are used for the slurry transportation. Slurry can be transported either pneumatically or hydraulically. These are different to each other on the basis of types of fluid which is used for transfer and also the nature of suspension of the solid particles in different continuum media. Solid mixed first and then transported to the destination for utilization purposes. The transportation of solids over long distances through pump is most of the times more economical compared to any other mode of transportation.

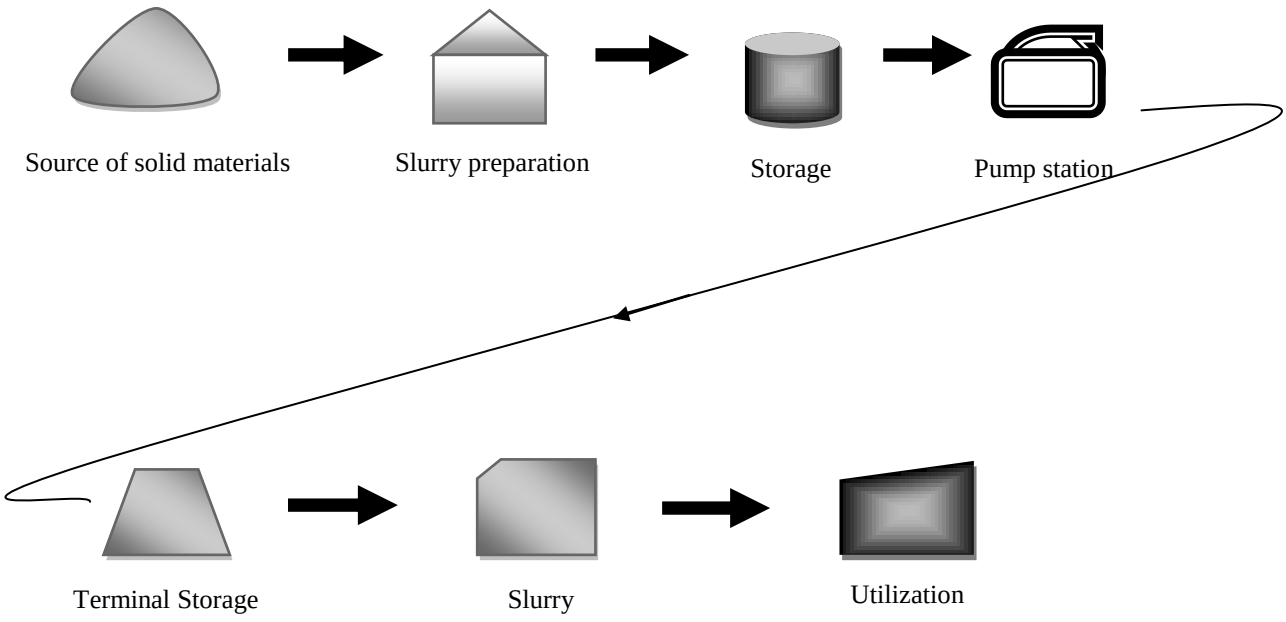

Figure 1.8: Transportation of slurry

The selection of slurry pumps mainly depends on the practical considerations rather than the economical concerns of efficiency. The two important factors on which the selection of pump depends are pressure discharge and abrasivity. Lots of pumps of different kinds are used for slurry transportation purposes but most important and common types of slurry pumps are the centrifugal slurry pump. Centrifugal pumps are cheaper, occupy less space and have lower maintenance costs than the positive displacement types and can handle much large solids. Slurry transportations pumps are used widely in the mining industry and for the ash disposal in the thermal power plants.

1.5 ROLE OF COMPUTATIONAL FLUID DYNAMICS IN PUMP DESIGN

Computational fluid dynamics (CFD) is an advanced computer-based design and analysis technique. A computational model is designed using CFD. CFD uses Numerical methods to solve the fundamental nonlinear differential equations.

Computational Fluid Design has become very popular approach for designing the such complex geometry. Design can be improved by analysing arrangements of multiple geometry using an identical set of simplification. A better performance can be obtained with the mathematical and computational error and using these resources in different manners accuracy can be imoroved using larger number of elements and due to this techniques results obtained in a very short time.

CFD improve flow characteristics as well as auditory characteristics of turbomachinery. A step-by-step computation was done to obtain an analytical solution. CFD analysis is important for the pump to improve the pump characteristics with hydraulic efficiency. Hydraulic characteristic can improve by applying proper boundry conditions, generates best quality of elements and chosing best turbulence model. There are many boundry conditions available which applied to inlet and outlet of pump. Pump inlet and pump outlet is defined at the face of the volume of the pump in the boundry conditions. The number of elements which generated by CFD software is depend on the memory of the computer which is used for analysis purpose. The generated elements for solution domain influences the solution of pump. Ideally,Depth analysis can be done by CFD and understabding the source of pulsation to decreases them during the pump operation. Because a customer want a fast and better solution for any problem. By the CFD analysis, poor area of design can be found due to this a vortex develop in the casing and for minimize this problem in flow, a modification was done. The coarse grid give better similarity with experimental results within a short time period and in tangential velocity component, a largest error was found. CFD analyses produce the results with better accuracy.

1.6 APPLICATIONS OF CFD

Computational fluid dynamics is used to analyze the flow of fluid, heat transfer and chemical reactions of the system with the help of computer-based simulation. Some main applications of CFD are as follows:

- Hydrodynamics of ships
- Aerodynamics of aircraft
- Combustion in IC engines and gas turbines
- Chemical process engineering
- Marine engineering
- Environmental engineering
- Automobile and Engine applications
- Industrial manufacturing applications
- Civil engineering applications
- Sports

1.7 MOTIVATION OF THE PRESENT WORK

Flow conditions inside the centrifugal pump can be visualized by numerical simulation and give the important information about the hydraulic design of a centrifugal pump. In the design of the centrifugal pump, a great improvement must be achieved by CFD analysis. Design pump is analyzed completely by the CFD analyses. Aims of the current work are to improve the quality and previous work related to the design and performance of the pump. By the parametric study, the effect of various pump geometry feature is investigated. Key parameter is taken from the literature survey to control the design process. They affect the pump performance. Those key parameters are listed below.

- Cutwater area of volute casing
- Variation in blade numbers

It is expected that the outcome of this thesis will provide a better understanding of the modification and the performance of the centrifugal pump.

CHAPTER 2

LITERATURE REVIEW

At present time, single and multistage centrifugal pumps are widely used in industrial and mining sectors. Centrifugal slurry pumps are used for handling different slurry mixtures. There are many design parameters for pumps, which affects the characteristics of pump immensely. To achieve better performance for a centrifugal pump, design parameters such as the number of blades for impeller-diffuser, blade angle, blade height and diffuser, blade width, impeller diameter and volute casing radius must be determined accurately, due to the complex liquid flow through a slurry pump. A lot of papers have been published on various aspects of wear in a slurry impeller or volute, performance corrections and derating, etc. The readers of these papers are often left with the impression that the design of these pumps is a combination of science and art. What are generally lacking in the research work are the guidelines for the design of centrifugal slurry pumps. The literature review of experimental and numerical evaluation of performance characteristics of centrifugal pumps are given in this chapter.

2.1 SIMULATION OF CENTRIFUGAL PUMP PERFORMANCE WITH WATER USING FLUENT

The performance of centrifugal pump has been evaluated to determine their dependence on various geometrical and dynamical parameters including the effect of variation in rotational speed and numbers of blades. Using computational simulation of fluid flow within the pump, the effect of geometrical modifications has examined in relation to pressure pulsations. Some literatures are as:

Minggao et al. (2009) have investigated the numerical research on performance prediction for centrifugal pumps. Commercial FLUENT software with standard k-ε model was used to simulate the performance of six centrifugal pumps models at design flow rate and off design flow rate for the improvement of performance and numerical calculation method. Every pump made run at different specific speed. They found an increment in the static pressure on

diffusion section at the volute outlet due to the small quantity of the flow rate while at big flow rate it decreases on the same place. Incident angle is negative for big flow rate and positive in small flow rate.

Karanth et al. (2009) carried out the numerical analysis on the effect of varying number of diffuser vanes on impeller-diffuser flow interaction in a centrifugal fan. FLUENT 6.3 with standard k-ε turbulence model was used for numerical analysis. They found that the static pressure recovery is better in odd number of diffuser than the even number. In volute casing static pressure reduction occurs when number of diffuser increased. Amplitude of static pressure fluctuations decreases at the exit flange when number of diffuser vanes increase.

Bacharoudis et al. (2009) investigated the parametric study of a centrifugal pump impeller by varying the outlet blade angle. Simulation is carried out using ANSYS FLUENT CFD Code with standard k-ε model. During the study of the impeller performance, blade outlet angle changed. The performance curve became smoother and flatter due to increase in the blade angle at whole range of the flow rates. Due to increase in outlet blade angle from 20^0 to 50^0, the increment in the head is more than 6 %. They obtained that at high flow rate, change in the head is more due to increase in the blade outlet angle. Hydraulic efficiency also increases due to increase the outlet blade angle.

Ozturk et al. (2009) have investigated the effect of impeller-diffuser radial gap ratio in centrifugal pump. The multi-purpose FLUENT with standard k-ε RNG model was used for simulation. A five backward curved blade impeller and nine vaned diffusers were used running at 890 rpm. Different radial gaps 10%, 15% and 20% was used and pressure fluctuations is maximum for 20% radial gap. They obtained that along front half of suction side, a significant increment is done in pressure fluctuation due to reduction in radial gap between impeller blade and diffuser vane. Pressure fluctuations are maximum at the trailing edge of the impeller blade.

Houlin et al. (2010) have analyzed the effects of blade number on the performance characteristics of centrifugal pump using CFD code FLUENT. During the simulation study number of impeller blade varies from 4 to7. They have analyzed the flow characteristics inside the pump with cavitation and non-cavitations conditions. As the number of blades

increase, head of the pump increases but the efficiency and NPSHR value decreased. They observed the impeller with 5 blades has the maximum efficiency.

Aman et al. (2011) have investigated the flow simulation and performance prediction of centrifugal pumps using CFD tool. They have used commercial CFD code ANSYS FLUENT 6.4 to simulate the six backward curved blade centrifugal pump using Standard k-ε turbulence modeling scheme. Flow was visualized in the centrifugal pump using 2-D simulation of turbulent fluid flow, including pressure and velocity distribution. They found that at small flow rate, blade inlet has the low pressure area at the suction side. As the flow rate increases, area gets closed at middle of the suction side of blade. Static pressure at small flow rate increases on diffusion section of the volute outlet while gets reduced at higher flow rate.

Jafarzadeh et al. (2011) analyzed the flow simulation of a low-specific-speed high-speed centrifugal pump. They have used commercial CFD code ANSYS FLUENT with Standard k-ε, RNG and RSM three turbulence modeling scheme for simulation to study the most suitable turbulence model. Flow was visualized in the centrifugal pump using 3-D simulation of turbulent fluid flow, including pressure and velocity distribution. Blade number varies from 5 to 7 and effect of number of blades was observed on the efficiency of the pump. They obtained that head coefficient was maximum for 7 number of blade impeller.

Yuan et al. (2011) have studied the flow numerical analysis within auxiliary-impellers of centrifugal pumps. ANSYS FLUENT with S.A turbulence model was used for numerical analysis. They obtained that the dynamic seals of auxiliary impeller influenced to flow through volute and main impeller. The auxiliary impeller centrifugal pump has high head than the pump without auxiliary impeller but it has lower efficiency. As the flow rate increases, the difference of head becomes large but the difference of efficiency becomes smaller.

Yang et al. (2011) have studied the flow distribution in the volute section of pump using CFD code FLUENT. The simulation study carried out with k- ε turbulence modeling scheme. The flow distribution was evaluated with different cross-section shape of the volute, throat area of volute and radial gap between volute tongue and impeller. When throat area

increases, pump efficiency drops in very small quantity. The maximum efficiency of the pump observed with round volute shape and spiral volute area.

Shojaeefard et al. (2012) studied the effect of changing the passage width of the impeller using CFD code FLUENT. The finite volume method was used for the discretization of the governing equations. The simulation study was performed using k -ε and SST turbulence modeling scheme. They found that the increasing of passage width of the impeller from 17 to 21 mm. The head and hydraulic efficiency increases due to reduction of the friction losses.

Chakraborty et al. (2012) studied the effects of number of blade variations on the centrifugal pumps performance at different rotational speeds using CFD code FLUENT. The number of blade varies from 4 to 12. The simulation study performed at different operating speed 2900, 3300 and 3700 rpm. They found that pump head and efficiency increases due to increase in rotational speed. Due to increase in the number of blade, total head developed by the centrifugal pump increases but the efficiency decreases. The optimum number of blade was found 10.

Chakraborty et al. (2013) analyzed that with variation of number of blade what changes on the performance of centrifugal pump. Number of blades varies from 5 to 7. Study mainly focus on the efficiency of the pump and evaluated at 3000 rpm with the help of ANSYS FLUENT 6.3 software with k-ε turbulence modeling scheme. They found that the centrifugal pump efficiency changes according to the blade number and it has maximum value for 7 blade number. Static pressure moderately increases from impeller inlet to the outlet. Due to increase in blade number, Static pressure increases all the time at the outlet of the volute.

Ozturk et al. (2013) have studied the effect of impeller-diffuser radial gap ratio in a centrifugal pump. ANSYS FLUENT software with standard k- ε RNG model was used. Nine vaned diffuser and five backward curved blade centrifugal pump was used which run at 890 rpm. At different flow rate results were represented for three different radial gaps (10%, 20%and 30%). Finally, Results were more accurate at 20% radial gap for pressure fluctuations. They obtained that due to reduction in radial gap between impeller blades and diffuser vanes, a significant rises in the pressure fluctuations along the front half of vane of

suction side. The magnitude of these fluctuations reached to peak point, when volume flow rate is large. Blade pressure fluctuations were largest at trailing edge of the impeller blade.

Hussein et al. (2013) have investigated the effect of rotational speed variation on the static pressure in the centrifugal pump. ANSYS/ FLUENT software with standard k-ε turbulence modeling scheme were used to analyze the effect of rotational speed on the static pressure. The study was done with five twisted blade centrifugal pump. A single blade passage gives the more fine results for the static pressure contour. They found that at high rotational speed, the static pressure contour gives negative low static pressure at the suction side of the blade, hub and shroud. Pressure reduces at the suction side when rotational speed increases.

2.2 SIMULATION OF CENTRIFUGAL PUMP PERFORMANCE WITH WATER USING CFX

Luo et al. (2008) have studied the impeller inlet geometry effect on performance improvement for centrifugal pumps. ANSYS CFX with RNG k-ε turbulence model and VOF cavitations model was used for flow analysis. They found that due to increase in the blade leading edge and blade angle at the inlet of the impeller, performance of the pump improved. If the inlet angle of the impeller is much larger then it improves the cavitations performance of the pump and leading edge affect for improves the hydraulic performance.

Spence et al (2009) have investigated the effect of geometrical variations on performance characteristics of a centrifugal pump. They have used the CFD code TASCflow to investigate the time variation pressure pulsation in the centrifugal pump. The pressure pulsations were evaluated at fifteen different location of the pump with three mass flow rate conditions. They observed that the transient flow simulation results show reasonable closure with the experimental result.

Ge et al. (2012) have studied the efficiency calculation and the vortex characteristics research of centrifugal pump. ANSYS CFX software with standard k-ε modeling scheme was used for simulation. In case of the small discharge, the difference between unsteady and steady calculation efficiency is comparatively large while in the large discharge, efficiency of

both is just close and as the discharge increases, the difference reduces. If the discharge is less than the optimal efficiency discharge then Steady calculation head is less than the unsteady calculation head and on the other hand when discharge is greater than the optimal efficiency discharge, calculation head of steady state is larger than the calculation head of unsteady state.

Hedi et al. (2012) analyzed the simulation study and three-dimensional numerical flow in a centrifugal pump. ANSYS CFX with k-ε turbulence modeling scheme was used to describe the turbulent flow process. Inside the vaneless impeller and volute CFD analysis, viscous Navier-Stokes equations used to simulate the flow for design purposes of the centrifugal pump. To obtain the three-dimensional pressure and velocity distribution, a solution method is developed within the centrifugal pump. By this method a fully elliptic partial differential equation can solve for the conservation of mass and momentum.

Jin et al. (2012) have investigated the effect of variation of the cross-sectional area of spiral volute casing for centrifugal pump. ANSYS CFX 13 with SST turbulence model was used for numerical analysis. They found that if the above-mentioned design parameters change, there will be the variation of a performance curve. Static pressure head increases with low flow and velocity head increases at high flow. The total head at low flow condition is almost uniform in circumferential direction and at higher flow the shape of curve becomes bent such as an arrow.

Zhou et al. (2013) have studied on the performance optimization in a centrifugal pump impeller by orthogonal experiment and numerical simulation. ANSYS CFX 13 with SST k-ω turbulence model was used. For research point of view five main geometric parameter of the impeller were chosen. 16 impeller were designed and then these 16 impeller were assembled with same volute and simulated with same numerical methods. And finally, the parameter was taken at which the efficiency is maximum. They found that the outlet width of the impeller has more effect on the head and efficiency.

Kaewnai et al. (2013) have investigated the flow through a double- acting impeller with a straight radial blades using CFD. ANSYS CFX 13 code with k-ε turbulence modeling scheme was used for simulation. Calculations were done for various dimensions of double

acting isolated impeller and impeller-collector assembly which are followed by three-dimensional drawing and domain specification. As the flow rate is reduced, Q-H curves increases continuously towards shut-off because circulation reduced between blade passages of the impeller. At the tongue region of the collector, pressure distribution is high.

Carrier et al. (2013) carried out the numerical investigation of a first stage of a multistage centrifugal pump impeller, diffuser with return vanes and casing. ANSYS CFX code with standard k-ε turbulence model with continuity and Navier-Stokes equations was used for numerical analysis. They found that the impeller blade height, diffuser vane height, number of impeller blades, diffuser vanes and diffuser return vanes and wall roughness height affect the brake horse power, efficiency and pump head in strong but different manner. Higher wall roughness heights of impeller and diffuser have negatively effect on the head, brake horsepower and efficiency.

Si et al. (2014) have studied the numerical investigation of pressure fluctuation in centrifugal pump volute based on SAS model and experimental validation. ANSYS CFX 14.5 software with SST k-ω turbulence model was used for simulation. Near the tongue region, pressure fluctuation intensity is strongest and distribution is irregular in the pump casing. At the cross-section of the volute casing, pressure fluctuation is symmetrically distributed. Dominant frequency of the monitoring points within the volute is indicated by the blade passing frequency and its multiples. During the off design conditions the low-frequency pulsation increases in the shaft component with small flow rate because vortex wave increase at off-design condition.

2.3 TWO PHASE FLOW SIMULATION THROUGH CENTRIFUGAL PUMP

Centrifugal slurry pumps have been concluded to evaluate the performance characteristics and to determine their dependence on various parameters including the effect of solids concentration, viscosity and density. It is important to consider experimental investigations involving pumps in addition to numerical studies, different flow regimes in solid-liquid flow

are discussed. A lot of papers have been published on two phase flow. Some of them is used for literatures which are as given below:

Yassine et al. (2010) carried out the experimental investigation for centrifugal slurry pump performance. To investigate the centrifugal pump performance, sand concentration varies from 0 to 15 % by weight. Test rig is used to inspect the flow behavior of different sand/water mixtures of 50 mm diameter PVC pipes with different fitting and valves. At the suction and delivery lines of the pump, pressure taps provided to measure the total head developed by the pump. Pump total manometric head, overall efficiency and electric power is measured for every experiments. It is analyzed that the head and efficiency are lower with slurries in comparison to the water due to present of the solid particles. As the sand concentration increases, the head and efficiency decreases while the power consumption increases at higher rate with increase in concentration of the sand than the rate of increase of the mixture specific gravity. Head ratio, efficiency ratio and power ratio do not vary with the flow rate.

Pagalthivarthi et al. (2011) carried out the CFD predictions of dense slurry flow in centrifugal pump casings. Eulerian multiphase model using k-ε was used with Eulerian-Eulerian approach in FLUENT 6.1 software. The effect of solid velocities, concentration and stresses was determined by parametric analysis with various operational geometric conditions of the pump. First shear stress of wall is calculated and then presented with the solid velocity and concentration along the wall of casing. They found an increment in solid concentration and shear stress of solid wall from upstream of the tongue region to the downstream of belly region.

Yi et al. (2011) have studied abrasion characteristic analyses of solid-liquid two-phase centrifugal pump. FLUENT code with RNG k-ε turbulent model was used for simulation. The effect of the solid phase on the abrasive performance of centrifugal pump is very small when the volume fraction is less than the 2.5% but the characteristic of wear is affected greatly. Due to reduction in the blade outlet angle, wear characteristic can be optimized. They suggested some modification in the design by changing the blade angle and then improved pump is compared with the original pump. They found that mixture density and shear stress both decrease but wear condition of the blade is improved.

Zhao et al. (2012) carried out the numerical investigation of solid–liquid two phase flow in a non-clogging centrifugal pump at off-design conditions. ANSYS FLUENT 6.4 with standard k-ε turbulence model was used. They found that particle starts to gather on pressure side of the impeller and most of the particle crash, due to increase in the particle diameter. As the sand volume fraction decreases at the inlet, particles start to accumulate on suction side of the impeller. They obtained that the inlet sand volume fraction has less influence than the diameter of the particle in whole channel of the pump. Finally, it is observed that the capacity of water transportation increases with the flow rate.

Wang et al. (2012) studied the solid-phase particles effect on the performance characteristics of pump using CFD Code FLUENT. They found that for the same particle size, the head decreases and shaft power increases due to increase in concentration of solid phase. They also observed that very low solid-phase concentration at the pressure side and high solid-phase concentration on the suction side of the pump.

Liu et al. (2012) studied the pattern of solid-liquid two-phase distribution in chemical process pump. The two phase simulation study was performed using mixture model and k -ε turbulence modeling scheme. They found that due to increase in the initial particle concentration, distribution of the solid phase changes. The concentration near the back side of the impeller was higher than the face side.

Yi et al. (2012) performed the numerical simulation of two phase solid-liquid characteristics on the centrifugal pump performance. They have compared the numerical result with the experimental data. The two-phase numerical simulation was carried out with different solid particle diameter and mixture concentration. They found that the influence of the solid phase characteristics is the function of flow rate. The best efficiency point of the pump also shifted with increase in solid particle diameter and volume fraction.

Yuliang et al. (2013) have studied on numerical simulation and analyzed of solid liquid two phase flow. A centrifugal pump of low specific speed was used to simulate the two phase flow. Two phase mixture model with RNG k-ε model was used for simulation. Particle density has less impact on the performance of the pump as compared to concentration and diameter. They found that the pump head and efficiency decreases due to increase in the

particle diameter and concentration. Volute tongue becomes strong when the solid phase has high concentration. When size of particle diameter is less than 0.05mm, pump has more accurate hydraulic performance.

Cheng et al. (2013) have studied the numerical research on the effects of impeller pump-out vanes on axial force in a solid-liquid screw centrifugal pump. RNG k-ε model was used for simulation. Six different screw centrifugal pumps by changing the impeller width and outlet vane were used. Solid volume fraction was calculated for each pump at different particle diameter and the different concentration. Pump-out vanes can change the magnitude and direction of the axial force. Due to increase in pump-out vanes number and width, axial force of the impeller increased. As the volume fraction of solid increases, axial force also increases.

Kumar et al. (2013) have studied the centrifugal slurry pump performance using CFD code FLUENT at design and off-design conditions. Steady state simulation with Moving Reference Frame (MRF) model was used to consider impeller-volute interaction. Different turbulence models namely, standard k- ε, RSM, k- ώ and RNG k- ε are applied for simulation of flow through the pump, which show reasonably close prediction of head–flow characteristics of pump by k-ε model. Performance characteristics of the pump is numerically predicted at four different operating speeds namely 1000 rpm, 1150 rpm, 1300 rpm and 1450 rpm with water. The numerical results are compared with the experimental measurements. The comparison indicates that the specific head, specific power and efficiency characteristics prediction are within an error band of 5 %. Simulation results showed that standard affinity relations are applicable to the slurry pump also.

CHAPTER 3

PHYSICAL AND RHEOLOGICAL PROPERTIES OF MATERIALS

Following three materials have been collected from different location used for the present study which is given below:

Coal collected from Assam Power Plant in Namrup (Disburgarh) district. Limestone collected from Sanu Limestone Unit in Jaislamer (Rajasthan). Zinc tailing collected from the operating plant at Rampura-Agucha mines of Hindustan Zinc Limited in the Bhilwara district of Rajasthan. Representative samples of each material were collected using standard cone and quarter method to study some of their important physical properties such as specific gravity, particle size distribution and rheological properties.

3.1PHYSICAL PROPERTIES OF COAL, LIMESTONE AND ZINC TAILINGS

Physical properties of coal, limestone and zinc tailings such as specific gravity, particle size distribution are calculated.

Particle Size Distribution

The PSD of a material can be important in understanding its physical and chemical properties. The strength and load-bearing properties of rocks and soils are affected by it. There are two methods i.e. sieve analysis and hydrometer analysis which are used to get this distribution. The most easily understood method of determination is sieve analysis. In sieve analysis, the sample is shaking in sieves and the sample should be properly dried. The sample which retained on each sieve is collected and using standard procedure, percentage retained on each sieve is calculated. The PSD is usually determined over a list of size ranges that covers almost all sizes which are present in the sample. Physical properties of coal,

limestone and zinc tailings depend upon their quality. Physical properties such as particle size distribution and specific gravity of coal, limestone and zinc tailings given in Table 3.1.

Table 3.1 Physical properties of coal, lime stone and zinc tailings

(a) Particle size distribution (PSD) of coal

Particle size, µm	355	250	150	106	75	53	37	21	8	3
% finer	100	94.47	89.15	83.21	78.19	72.86	55.73	41.07	30.89	20

(b) Particle size distribution (PSD) of lime stone and zinc tailings

Material	**Particle size, µm**	250	150	106	75	53	37	21	8
Lime stone	**% finer**	100	94.93	89.34	77.47	63.78	53.25	34.43	17.08
Zinc tailings	**% finer**	100	94.93	89.34	80.27	69.59	56.86	36.23	17.08

(c) Specific Gravity of solids is calculated using

$$\text{Specific gravity} = {}^{(W_{bs} - W_b)}\big/_{\{W_{bw} - W_{bsw} + (W_{bs} - W_b)\}}$$

W_{bs} = weight of beaker and solid

W_b= weight of beaker

W_{bw}= weight of beaker and water

W_{bsw}= weight of beaker, solid and water

Weighted mean diameter (d_{wm})

The differential analysis of the size distribution was done and weighted mean diameter of different samples was calculated using following equation:

$$d_{wm} = \sum_{i=1}^{N} f_i \, d_i$$

Where N is the number of size groups in which the total sample was divided.

Material	**Specific gravity**	**Particle size µm**	
		d_{50}	**d_{wm}**
Coal	1.47	31	56.96
Limestone	2.23	33	49.51
Zinc tailings	2.76	33	46.83

3.2 SCANNING ELECTRON MICROSCOPY (SEM)

Electronic console and the electron column is the two main component of the Scanning Electron Microscopy (SEM) instrument. The electronic console provides control knobs and switches. SEM is a method where an electron beam is scanned over a surface of a sample placed in a vacuum chamber. The electrons from the beam are accelerated towards the surface. As the beam of electrons meets the surface secondary electrons or backscattered electrons are emitted from the surface. Secondary electrons are low-energy electrons and give information about the topography and surface variation of the sample.

Backscattered electrons are high-energy electrons which are emitted when an electron from the beam is elastically scattered at the core of the atom. This collision gives information about the elemental composition of the surface (Grolig et al. 2013). Figure 3.1 shows the 6510LV model SEM machine which is made by the JEOL company. In figure 3.2, figure 3.3 and figure 3.4 shows SEM of coal, limestone and zinc tailings at 500x Secondary electron images (SEI).

Figure 3.1: Scanning Electron Microscopy Machine

Scanning Electron Microscopy (SEM) images of Coal, Limestone and Zinc Tailings

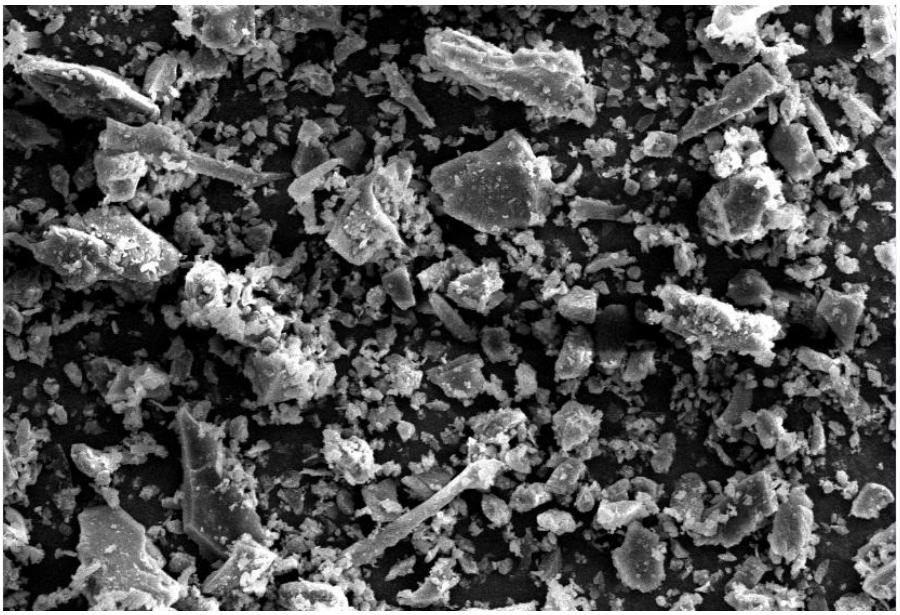

Figure 3.2: SEM of coal, 500x SEI

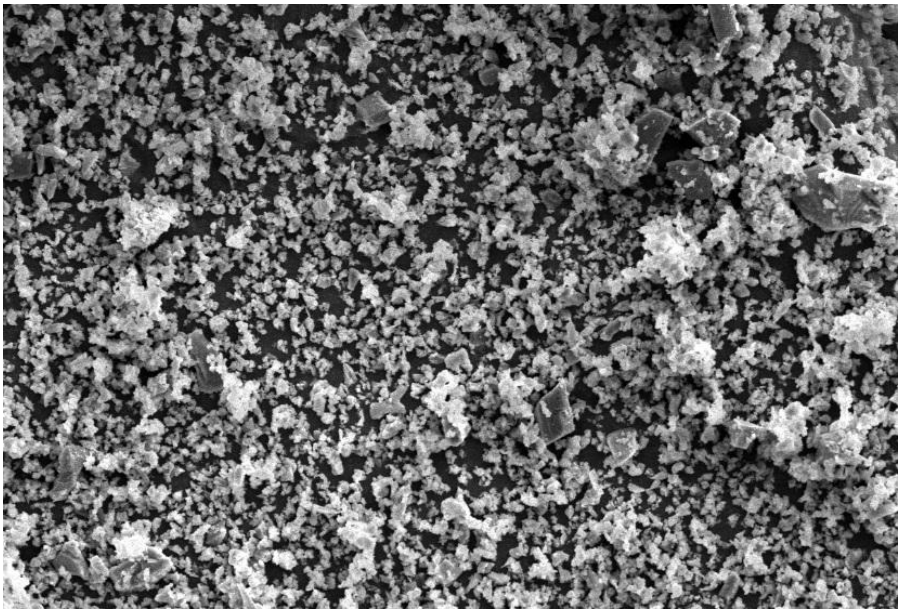

Figure 3.3: SEM of limestone, 500x SEI

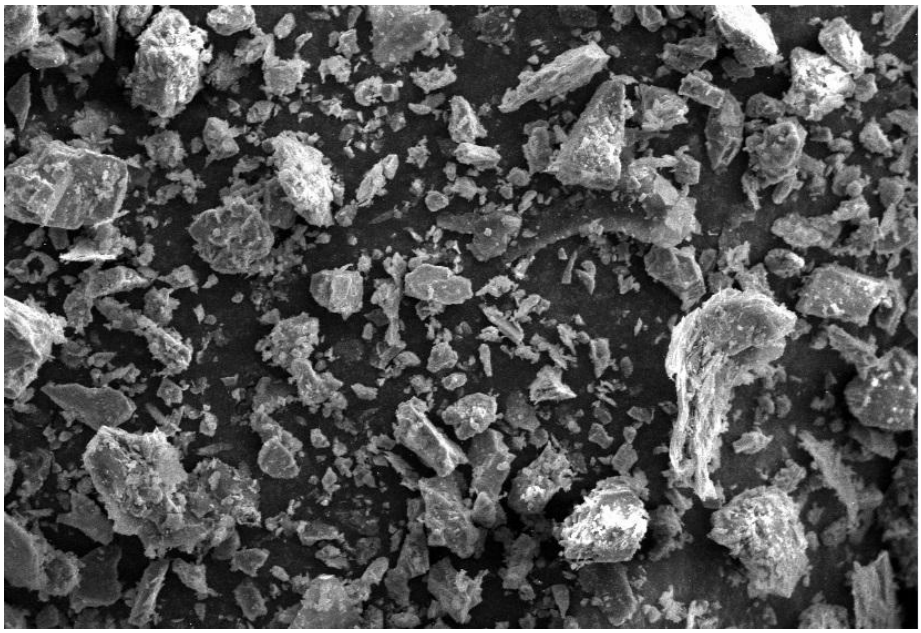

Figure 3.4: SEM of zinc tailings, 500x SEI

3.3 Energy Dispersive X-Ray (EDX)

EDX systems are attachments to Electron Microscopy instruments (Scanning Electron Microscopy (SEM) or Transmission Electron Microscopy (TEM)) instruments where the imaging capability of the microscope identifies the specimen of interest. INCA X- act model of EDX machine in Figure 3.1 is used which is made by the OXFORD instrument. The data generated by EDX analysis consist of spectra showing peaks corresponding to the elements making up the true composition of the sample being analyzed. The technique can be qualitative, semi-quantitative, quantitative and also provide spatial distribution of elements through mapping. The scanning electron microscope (SEM) is related to the electron probe, is primarily designed not only for producing electron images but also used for element mapping. It can be used for point analysis if an X-ray spectrometer is added. There is considerable overlap in the functions of these instruments. EDX of coal, limestone and zinc tailings are shown in figure 3.5, figure 3.6 and figure 3.7 which are given below:

Table 3.2 Energy Dispersive X-Ray (EDX) of Coal

Element	Weight %	Atomic %
$CaCO_3$ K	59.44	68.63
SiO_2 K	32.96	28.57
Al_2O_3 K	0.69	0.36
SiO_2 K	1.43	0.71
FeS_2 K	2.58	1.12
Cu K	1.84	0.40
Zn K	1.05	0.22
Totals	100.0	

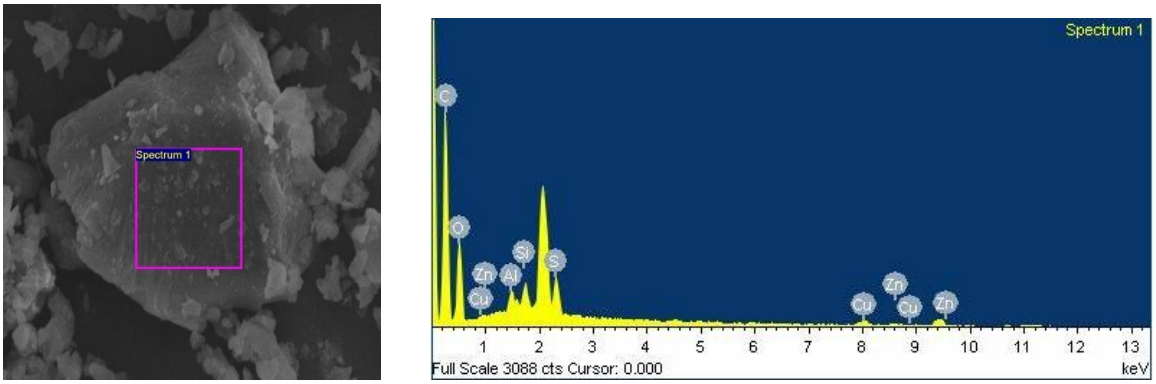

Figure 3.5 Energy Dispersive X-Ray (EDX) of Coal

Table 3.3 Energy Dispersive X-Ray (EDX) of Limestone

Element	Weight %	Atomic %
SiO_2 K	67.66	83.58
MgO K	1.48	1.20
Wollastonite K	30.86	15.22
Totals	100.0	

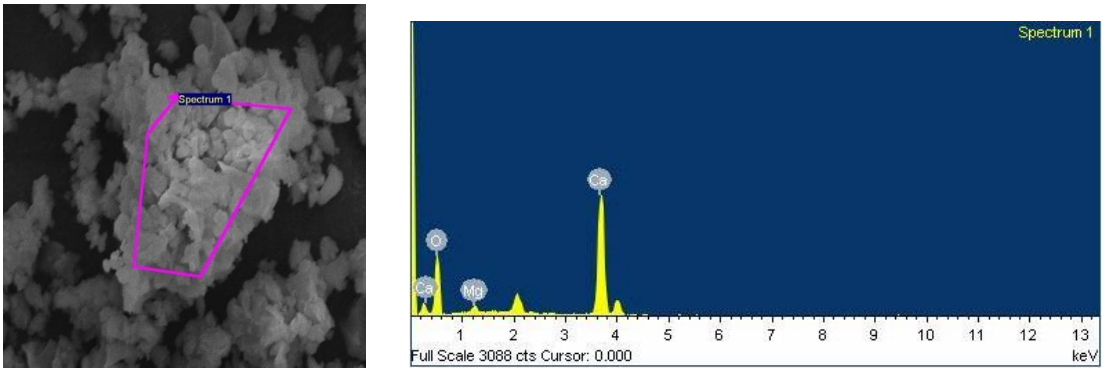

Figure 3.6 Energy Dispersive X-Ray (EDX) of Limestone

Table 3.4 Energy Dispersive X-Ray (EDX) of Zinc Tailings

Element	Weight %	Atomic %
$CaCO_3$ K	30.82	48.69
SiO_2	28.70	34.03
Al_2O_3 K	3.89	2.73
SiO_2 K	5.90	3.99
FeS_2 K	3.47	2.05
MAD K	1.67	0.81
Fe K	5.36	1.82
Cu K	2.24	0.67
Zn K	17.95	5.21
Totals	100.0	

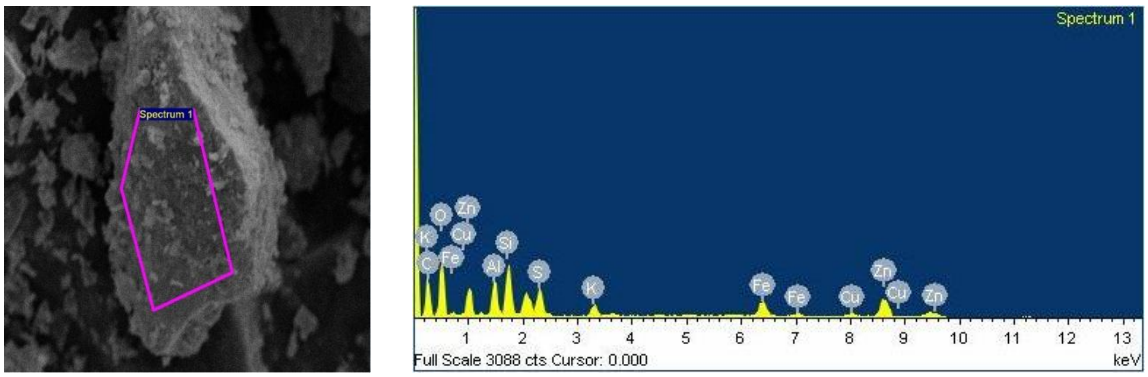

Figure 3.7 Energy Dispersive X-Ray (EDX) of Zinc Tailings

3.4 RHEOMETER

A rheometer is a kind of viscometer that measures visco-elastic properties of materials beyond just viscosity. Rheometer rheoplus is used for solid liquid suspension shown in figure 3.8. Before using the rheometer for testing purpose, bob and the cup assembly is fixed with the help of locking device. The Rheometer is used to calculate the rheological characteristics of the slurries. Rheology is the flow of fluids and deformation of solids under different types of stress and strain. Rheology of the solid-liquid suspension determine at the concentration range varying from 10 to 65 % (by weight) in environmental temperature 25^0 C. Rheological data are given in Table 3.5.

Figure 3.8: Rheometer

Table.3.5 Rheological properties of coal, limestone and zinc tailings

(a) Rheological Properties of coal at 25^0 C

Concentration (C_w) %	Relative viscosity	Water viscosity(cP)	Slurry viscosity(cP)	Flow behaviour
10	1.3	0.99	1.282	Newtonian
20	2.08	0.99	2.064	Newtonian
30	3.5	0.99	3.422	Non-Newtonian
35	5.01	0.99	4.9	Non-Newtonian
40	11.2	0.99	11.0913	Non-Newtonian
45	16.8	0.99	16.451	Non-Newtonian
50	52.8	0.99	51.483	Non-Newtonian
55	57.09	0.99	56.1013	Non-Newtonian

(b) Rheological Properties of limestone at 25^0 C

Concentration (C_w) %	Relative viscosity	Water viscosity(cP)	Slurry viscosity(cP)	Flow behaviour
20	1.2	0.99	1.342	Newtonian
30	1.7	0.99	1.835	Newtonian
40	2.3	0.99	2.272	Non-Newtonian
50	5.9	0.99	5.753	Non-Newtonian
55	8.7	0.99	8.582	Non-Newtonian
60	16.1	0.99	15.864	Non-Newtonian
65	56.02	0.99	55.135	Non-Newtonian

(c) Rheological Properties of zinc tailings at 25^0 C

Concentration (C_w) %	Relative viscosity	Water viscosity(cP)	Slurry viscosity(cP)	Flow behaviour
30	1.7	0.99	1.681	Newtonian
40	2.5	0.99	2.472	Newtonian
45	3.0	0.99	2.995	Non-Newtonian
50	4.4	0.99	4.358	Non-Newtonian
55	6.5	0.99	6.463	Non-Newtonian
60	11.2	0.99	10.978	Non-Newtonian
65	32.2	0.99	31.849	Non-Newtonian

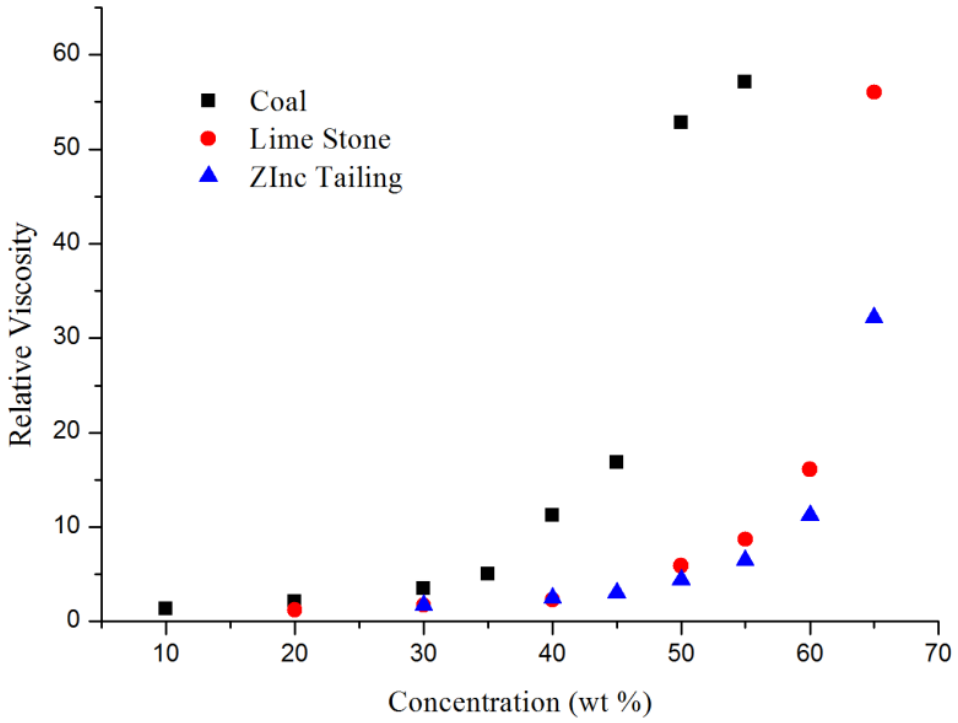

Figure 3.9: Relation of relative viscosity with concentration

CHAPTER 4

COMPUTATIONAL FLUID DYNAMICS

4.1 COMPUTATIONAL FLUID DYNAMICS

Computational fluid dynamics (CFD) is an advanced computer-based design and analysis technique. A computational model is designed using CFD and it represents as a device at which the study is focused. CFD is particularly related to the fluid which is in motion and how the behavior of fluid affects the heat transfer process and chemical reactions in combusting flows. General fluid flow equations are applied for estimate the flow field and related physical phenomena. The meaning of the computational part is to study the fluid flow using numerical simulation which use the computer programs or software packages performed on high speed digital computers to obtain the numerical solutions. Some CFD-based educational software packages are developed such as FlowLab by ANSYS and by Fluent the concept of fluid flow and heat transfer through a "Virtual Fluids Laboratory."

In 1960s for the aero-space industry, first CFD codes were developed. Modern high-speed aircraft Northrop F-20 use the CDF as a design tool for their complicated transonic aerodynamics flow patterns. Almost all CFD codes are based on the Navier-Stokes equations which come from the Newton's second law for fluid flow. Fundamental mathematical equations are used to describe the physical characteristics of the fluid motion in partial differential form which is generally called governing equations in CFD. Navier-Stokes equations are the basic governing equations for all types of fluid motion but these equations is solved for the laminar flow and for some simple geometry of turbulent flow. So many complex geometries of turbulent flows have to be solved numerically. Navier-Stokes equations have an exact numerically solution for the turbulent flow. Exact solution can be obtained only when the size of computational cells is smaller than the length scale of the smallest turbulent eddies but it is impractical for most of the cases. Time-averaged equations such as Reynolds-averaged Navier-Stokes equations (RANS) are used by CFD codes for this type of reason. Turbulent is modeled for sub-grid scales with this type of approach. Depending on the flow characteristics, many turbulent models are available.

4.2 DISCRETIZATION METHODS IN CFD

In discretisation process, the governing differential equations are transformed into their discrete counterparts. The discretization process can be identified with the help of some common methods which are in use today. The basics aspects of discretization methods are consistency, stability, convergence and conservation. The discretization handles the discontinuous solutions gracefully. Some discretization methods are given below:

Finite Difference Method

Finite-difference method is one of the oldest methods and it is simple to program. The geometric domain divided into discrete nodal points for developing numerical solutions. At every nodal points of the grid, the fluid-flow domain is described. Finite-difference approximations are generated using Taylor series expansions. At every point of grid, finite-difference approximations replaced partial derivatives and generate algebraic equations for the flow solution. In one-dimensional space a simple differential equation possesses a smooth analytical solution with simple boundary conditions. There is no need of uniform grid spacing between the nodal points but to maintain the accuracy, the amount of grid stretching must be in limits which can be imposed.

Finite Volume Method

The integral form of conservation equations are discretized by finite –volume method in physical space. Variable values are expressed into the centre values by the interpolation at the control volume and suitable quadrature formulae are used to approximate the volume and surface integrals. Finite-volume method does not work with the grid intersection but it does with the control volumes and any type of grid can be accommodated by it. Unstructured grid is often used instead of structured grid because unstructured grid allows a large number of options for the definition of the shape and the location of the control volumes. Boundaries of the control volume are defined by the grid.

Finite Element Method

The distinguishing feature of finite element method is that simple piecewise polynomial functions are used by it on the local elements so that the variations of the unknown flow variables can be described. The error associated with the approximate functions measured using the concept of weighted residuals which are later minimized. The flow solution is obtained for the unknown terms of the approximating functions by solving the set of nonlinear equations. The most significant advantage of the finite-element method is that arbitrary geometries can be handled by it.

4.3 PROCESS OF CFD ANALYSIS

CFD codes solved the fluid flow problem. All commercial CFD packages considered the sophisticated user interface to input problem parameters for providing the easy access to their solving power. CFD analysis is a complex task which involves three main stages:

1. Pre-processing

2. Solving

3. Post-processing

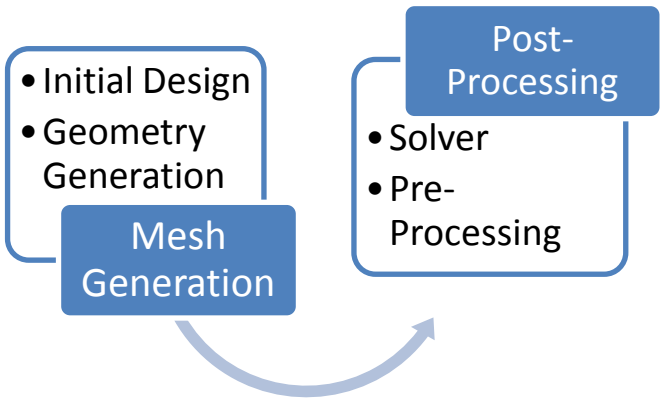

Figure 4.1: CFD Procedure

Pre-processing

Properties of the fluid acting on the domain are defined by the users before the starting of the analysis. Computational fluid dynamics is built by preprocessing.

- Formation of the flow problem

- Modeling and design the geometry
- Mesh Generation
- Explain the properties of the fluid material and boundary conditions for the model

Solving

A very less time is taken for solving the flow equations because flow equations are solved iteratively in all grid cells. The solution speed can increase when multicore computer clusters are used for calculation purpose. To obtain the accurate solutions of the partial differential equations, the results should be converged.

- Selection of the appropriate flow equations and numerical schemes
- Flow equations are solved until the predetermined convergence criteria obtained

Post-processing

Post-processing is the last step in CFD analysis. It is used to visualize the results which are obtained from the solver.

4.4 MULTIPHASE FLOW

Multiphase system is very complex because there are various phases in it. Multiphase flow investigations are intense research in the climate of significant advancements being achieved in computing power and performance. The boundary condition in multiphase system is applied for each single phases. To solve the multiphase system is very difficult. Low overall efficiency and severe abrasion are the two main problems exist in two phase flow. The most important parameters which influence most to the centrifugal pump performance are concentration, diameter and density of the particles. Some engineering application of multiphase flows are, gas bubbles in liquid or liquid droplets in gas, fluidized bed combustion and liquid fuel injected as a spray in combustion machines.

The two main approaches for the numerical calculation of the multiphase flow: “Eulerian-Lagrange approach and Eulerian-Eulerian approach”.

4.4.1 Eulerian-Lagrangian Approach

Momentum, mass and energy can be exchanged by dispersed phase with the fluid phase. The dispersed phase is solved when a large number of particles, bubbles or droplets tracked through a calculated flow field, while the fluid phase is treated as a continuum by solving the time-averaged Navier-Stokes equations. In this model, a fundamental assumption is made in which a low volume fraction is occupied by dispersed second phase but high mass loading is acceptable.This approach gives the complete information about the behavior and residence time of the individual particles. The Lagrangian-Eulerian approach is mostly used for the simulation of multiphase flows.

4.4.2 Eulerian-Eulerian Approach

In this approach, every phase is treated mathematically as interpenetrating continua. The volume of one phase cannot be absorbed by the other one. Volume fractions used in the solid phase are assumed to be continuous functions of space and time and their sum should be equal to one. A set of equations is obtained to derive the conservation equations for each phase which have the same structure for all phases. Three different Eulerian-Eulerian multiphase models are available: volume of fluid model, mixture model, eulerian model.

4.4.2.1 Volume of Fluid Model

In the VOF model, fluids share a single set of momentum equations and the volume fraction of all the fluids are tracked throughout the domain in each computational cell. Some applications of the VOF are: “stratified flows, free-surface flows, filling, sloshing, the motion of large bubbles in a liquid, the motion of liquid after a dam break and the steady or transient tracking of any liquid-gas interface”. It is a surface-tracking technique which is applied to a fixed Eulerian mesh.

4.4.2.2 Mixture Model

It is the model which is designed for more than one phases. Mixture model also treats the phases as the interpenetrating continua. To described the dispersed phases, mixture momentum equation and prescribes relative velocities are solved by the mixture model.

Homogeneous multiphase flow is modeled by mixture model when mixture model is used without relative velocities for the dispersed phases. Continuity and momentum equations are used in mixture model in the forms as (Zhao et al. 2012).

The continuity equation

$$\frac{\partial}{\partial t}(\rho_m) + \nabla.(\rho_m \vec{v}_m) = 0 \qquad \text{….. (3.1)}$$

The momentum equation

$$\frac{\partial}{\partial t}(\rho_m \vec{v}_m) + \nabla.(\rho_m \vec{v}_m \vec{v}_m) = -\nabla p + \nabla.\left[\mu_m\left(\nabla \vec{v}_m + \nabla \vec{v}_m^T\right)\right] + \rho_m \vec{g} + \vec{F} + \nabla.\left(\sum_{k=1}^{n} \alpha_k \rho_k \vec{v}_{dr,k} \vec{v}_{dr,k}\right) \qquad \text{….. (3.2)}$$

The sliding velocity $\vec{v}_{qp}$ has a relation with the drift velocity $\vec{v}_{dr,p}$ as (Zhao et al. 2012)

$$\vec{v}_{dr,p} = \vec{v}_{qp} - \sum_{k=1}^{n} \frac{\alpha_k \rho_k}{\rho_m} \vec{v}_{qk} \qquad \text{….. (3.3)}$$

The solid volume fraction equation (Zhao et al. 2012)

$$\frac{\partial}{\partial t}(\alpha_p \rho_p) + \nabla.(\alpha_p \rho_p \vec{v}_m) = -\nabla.(\alpha_p \rho_p \vec{v}_{dr,p}) \qquad \text{….. (3.4)}$$

4.4.2.3 Eulerian Model

Eulerian model is one of the most complex models of the multiphase. For each phase, a set of 'n' momentum and continuity equations are solved by it. Main applications of this model are as: bubble columns, particle suspension and fluidized beds. The properties for granular flows are obtained from the application of the kinetic theory. Eulerian model is computationally intensive among the multiphase models.

4.5 TURBULENCE MODELS

Turbulence occurs in the flow field due to the irregular and random motions of the particles. Turbulence mainly occurs when the inertia force become more significant than the viscous

force in the fluid. High Reynolds Number is used to characterize the turbulence. Without any need of additional information, laminar and turbulent flows are described by the Navier-Stokes equations. Variable is divided into two components in turbulent flow, one is time-averaged part which is independent of time and second is fluctuating part. When the turbulence is in small scales, direct numerical simulation of turbulence is very expensive computationally because it requires a very small finite volume meshes for simulation. To solve this problem, the governing equations are modified and manipulated. Due to this, several unknown variables are related with these modified equations and hence, unknown variables are determined by the turbulence models.

Turbulence models consist of randomness in the flow field with time and space. Turbulence model is mainly 3D. Two turbulence models which are most common ; classical models and large eddy simulation.

4.5.1 K-ε Turbulence Model

The standard k-ε model is a semi empirical two-equation model. A standard k-ϵ turbulence model was used for the turbulent multiphase flow. The turbulent velocity and length scales are obtained by solving the two different transport equations (turbulence kinetic energy and its dissipation rate). The turbulence quantities are calculated in k-ε mixture turbulence model. The mixture model is used where the k and ε equations are solved and the physical properties of the mixture are adopted. The assumption of an isotropic eddy viscosity in the standard k-ε model is the main weakness. The k-ε model is used for industrial applications due to its robustness and simplicity.

4.5.2 K-ω Turbulence Model

In the K-ω model, two transported variable is used in this model, one is turbulent kinetic energy ‘K’ and the second is specific dissipation ‘ω’. The scale of the turbulence is determined by the specific dissipation while the K determines the energy in the turbulence.

Following equation can be used to calculate the Head and Power output of the pump using simulation result:

Calculation of Head (H_{Total}):

$$H = \left(\frac{P_2}{\rho g} + Z_2\right) - \left(-\frac{P_1}{\rho g} - Z_1\right) + \frac{V_2^2}{2g} - \frac{V_1^2}{2g} \quad \text{..... (3.5)}$$

Or

$$H = \frac{P_{out} - P_{in}}{\rho g} \quad \text{..... (3.6)}$$

Power output:

$$P_o = \rho g Q H \quad \text{..... (3.7)}$$

Total efficiency:

$T = F.r$

$P_i = T\,\omega$

$\omega = 2\pi N/60$

$\eta = P_o / P_i$ ..... (3.8)

4.6 GEOMETRY OF EXISTING CENTRIFUGAL PUMP

GAMBIT software 2.3.16 has been used for modeling the geometry of the existing model (with blade number 5). Fluent 6.3.26 simulation software has been used for single phase and multiphase analysis. A closed type impeller of Ni- hard material is used. Impeller eye width, eye diameter, outlet width and outlet diameter is 44.2 mm, 110 mm, 68.59 and 265 mm respectively. Impeller inlet and outlet vane angle in degree are 23 and 25. Single volute casing of Ni- hard material is used in existing model of pump. Volute width and base volute diameter are 85 mm and 275 mm. Inlet and outlet passage diameter are 100 mm and 50 mm respectively.

The existing centrifugal pump contains following three parts.

1. Impeller
2. Casing
3. Inlet Passage

The existing pump performance has been evaluated with water at operating speed 1450 rpm with water (Kumar et al. 2013). Same model has been extended to simulate the two phase

flow solid-liquid minerals suspension at 1450 rpm with different concentration. The solid concentration of minerals is used 30%, 40%, 50% and 55% by weight. Figure 4.2 shows the geometry of existing pump which was created with the help of Gambit software.

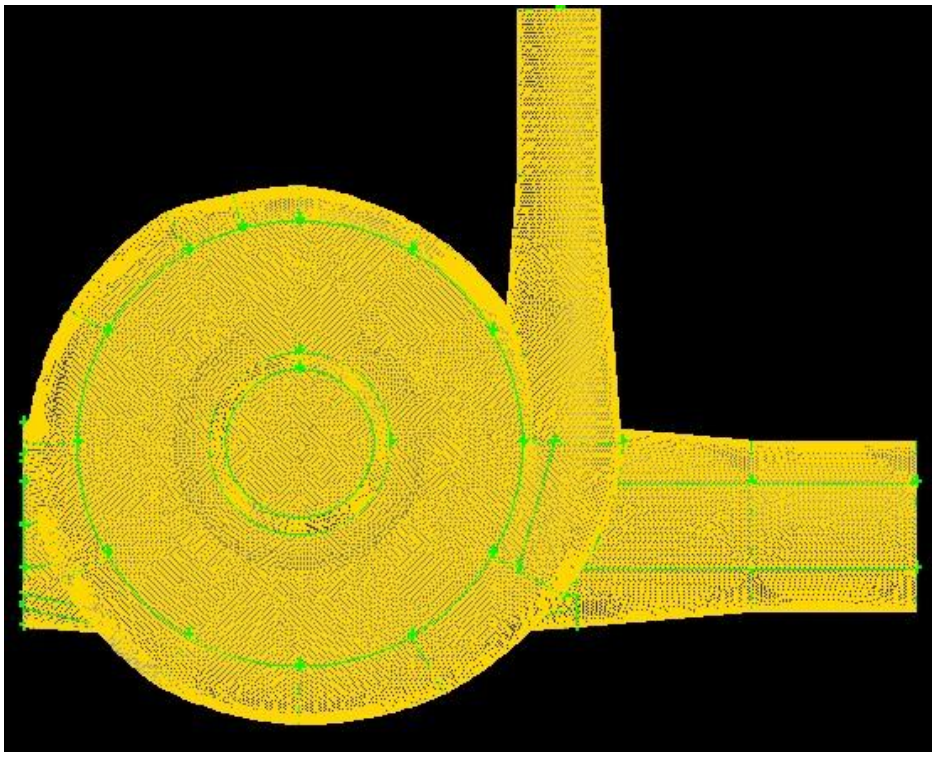

Figure 4.2: Existing centrifugal slurry pump

4.7 BOUNDARY CONDITIONS

The boundary conditions applied at different surfaces for all the models. A velocity inlet boundary condition is applied at the inlet of the pump. Same velocity is given to the both phase. First phase is water and second phase is slurry but in second phase volume fraction is given according to the concentration of the solid. Pressure outlet boundary condition is selected for the outlet of the pump. Rest of sections of the slurry pump is taken as walls. A no slip boundary condition is taken for the wall boundaries where the velocity of the stream increases from zero to the free stream velocity accordingly from the wall. The effect of the gravity is also considered in negative Y-axis direction. The Boundary conditions are given in Table 4.1.

Table 4.1: Simulation setup and Boundary condition for Two phase flow analysis

Category	Discription	
Model	Multiphase Model	i) Mixture model ii) No of phases : 2
	Viscous Model	i) k-ε turbulence, standard ii) standard wall function
Phase Properties and Interaction	Phase 1 (Primary)	Water
	Phasse 2 (Secondary)	Coal (Granular)
		Limestone, (Granular)
		Zinc talling, (Granular)
	Particle Diameter	31 µm (coal) 33 µm (Limestone) 33 µm (Zinc tailings)
	Granular Viscosity	Syamlal-Obrien
	Granular Bulk Viscosity	Lun-et-al
	Phase Interaction	Syamlal-Obrien
Operating Conditions	Operating Pressure	101325 pa
	Gravitational Acceleration	-9.81 m/s^2 in negetive y direction
Boundary Conditions	Inlet	Velocity inlet with constant value for both phases and volume fraction for secondary phase.
	Outlet	Pressure outlet with constant values
	Wall	No-slip at wall
Solution Control	Pressure Velocity Coupling	SIMPLE
	Momentum	First order upwind
	Volume Fraction	First order upwind
	Turbulent Kinetic Energy	First order upwind
	Turbulent Dissipation Rate	First order upwind

4.8 SIMULATION OF MINERALS SUSPENSION THROUGH CENTRIFUGAL SLURRY PUMP

Existing model has been extended to simulate the two phase solid-liquid minerals suspensions. Coal, limestone and zinc tailings are used for minerals. The two-phase flow in the existing pump is very complex. The Simulation has been conducted through the centrifugal slurry pump with different types of minerals suspension to investigate the effect of the minerals on the pump performance. The physical properties and rheological properties of the minerals have been discussed in Table 3.1and Table 3.2 respectively of earlier chapter and the ranges of parameters are given in table 4.2. The head, power and efficiency of the pump for different minerals have been measured at various flow rates. The performance of the pump has been evaluated at 1450 rpm with three different minerals namely coal, limestone and zinc tailings. The simulations were conducted with coal, limestone and zinc tailing at four concentrations by weight namely 30%, 40%, 50% and 55% respectively at 1450 rpm.

Table 4.2: Range of parameters for pump performance

Mineral	Concentration Range	Parameter Evaluated	Speed(rpm)
Coal	30 – 55%	Head developed , power and efficiency	1450
Limestone	30 – 55%	Head developed , power and efficiency	1450
Zinc tailings	30 – 55%	Head developed , power and efficiency	1450

4.9 SIMULATION OF MINERALS SUSPENSION

The solid-liquid two-phase flow is investigated by CFD simulations in existing pump at four different flow rate conditions. The static pressure and volume fraction contours of the coal, limestone and zinc tailings are examined in detail. In this section static pressure contours are

evaluated. Simulations of minerals are conducted at different flow rate and various concentrations by weight. The simulations of coal are conducted at four different flow rates

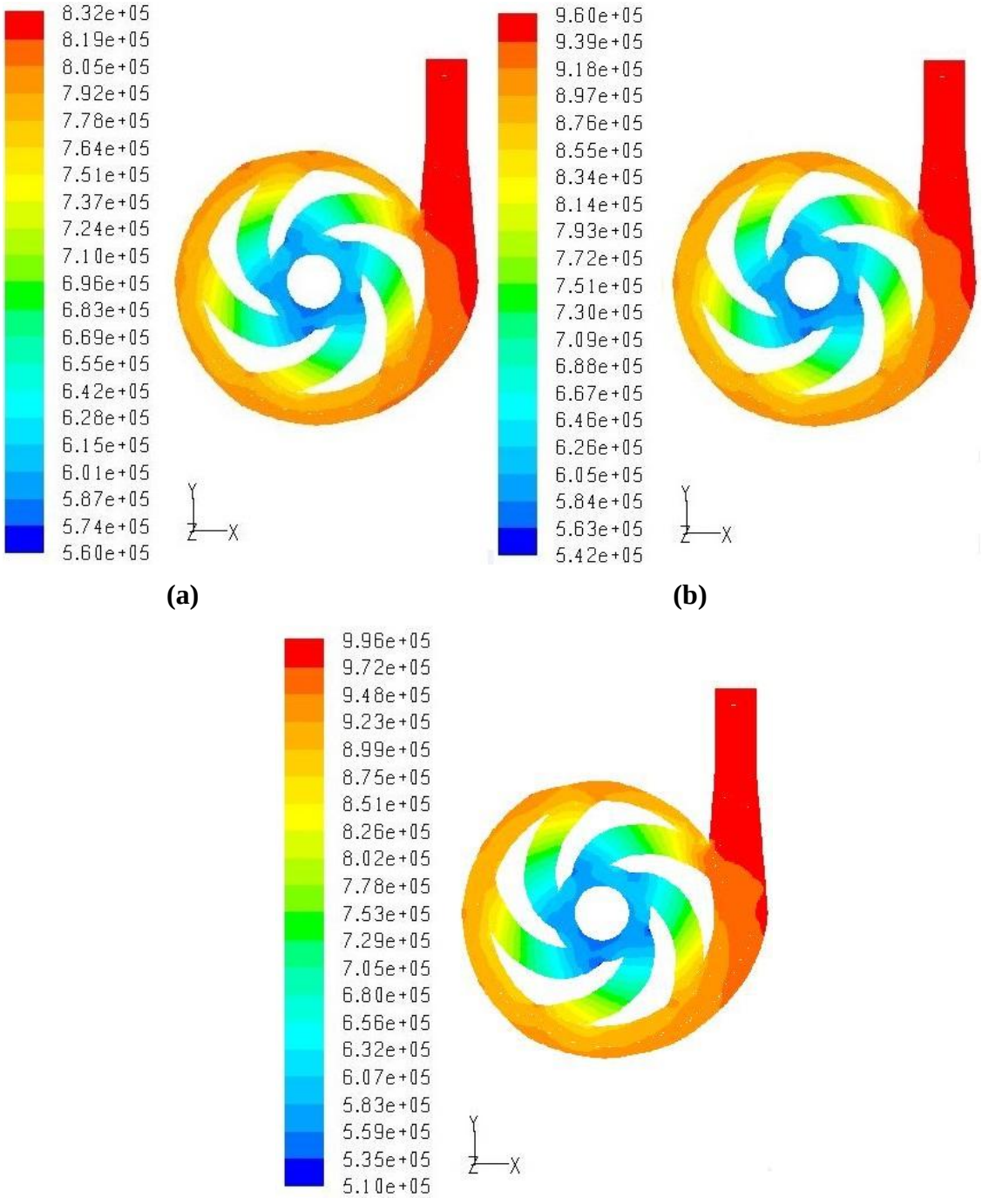

Figure 4.3: Contour of Static pressure (Pascal) for 30 % concentration (a) coal at 3.88 lps (b) lime stone at 6.14 lps (c) zinc tailings at 7.53 lps at 1450 rpm

3.88 lps, 5.83 lps, 7.78 lps and 9.73 lps. The simulations of Limestones are conducted at 6.14 lps, 9.20 lps, 12.29 lps and 15.36 lps flow rates, and flow rate for the zinc tailings are 7.53 lps, 11.29 lps, 15.07 lps and 18.83 lps. All simulations are conducted for three minerals (coal, lime stone and zinc tailings) at all flow rates and various concentrations means that one flow rate is used to simulate for four different concentration 30%, 40%, 50% and 55% at same rotating speed 1450 rpm. After the simulation with the help of some mathematical formulas the head, input power and efficiency is calculated. Minerals head decreases due to increase in mass flow rate. The head is maximum for small flow rate and minimum for the larger flow rate. As well as the concentration of the solid by weight increases the head and efficiency reduces but efficiency can be maximum for any one of them. Figure 4.3 show that the static pressure contours (Pascal) for coal, limestone and zinc tailings at 30% concentration. Head is maximum for all three minerals as compared to other but the efficiency is minimum. Head is maximum for coal as compared to the limestone and zinc tailings.

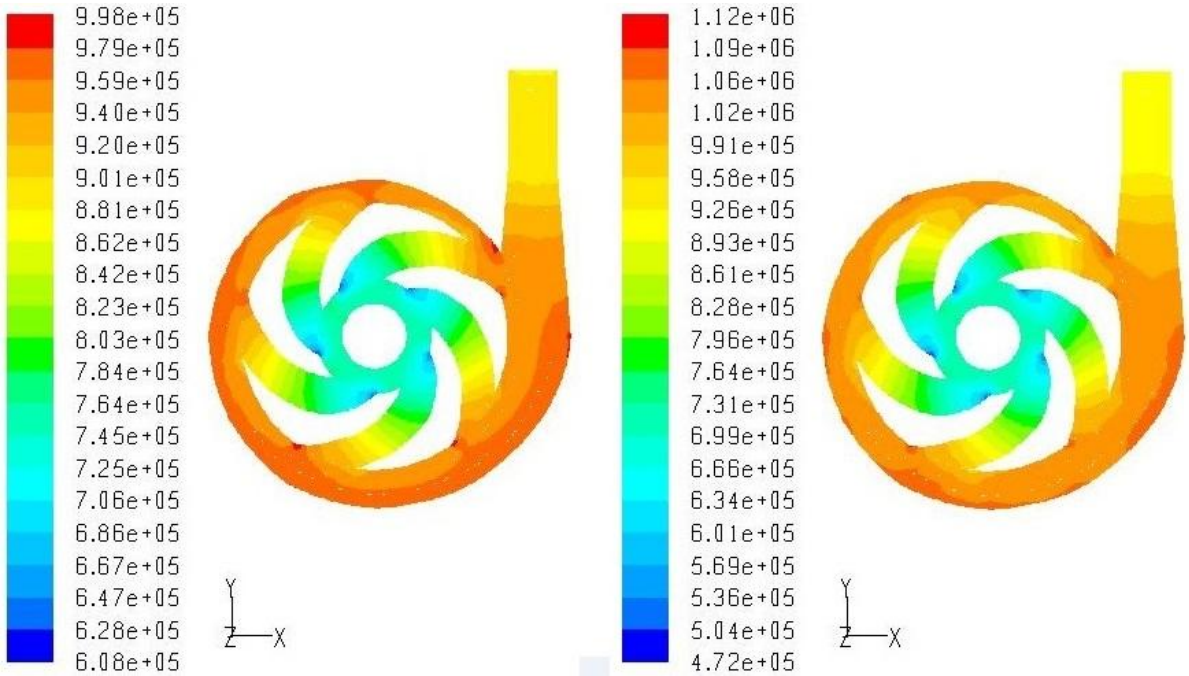

(a) **(b)**

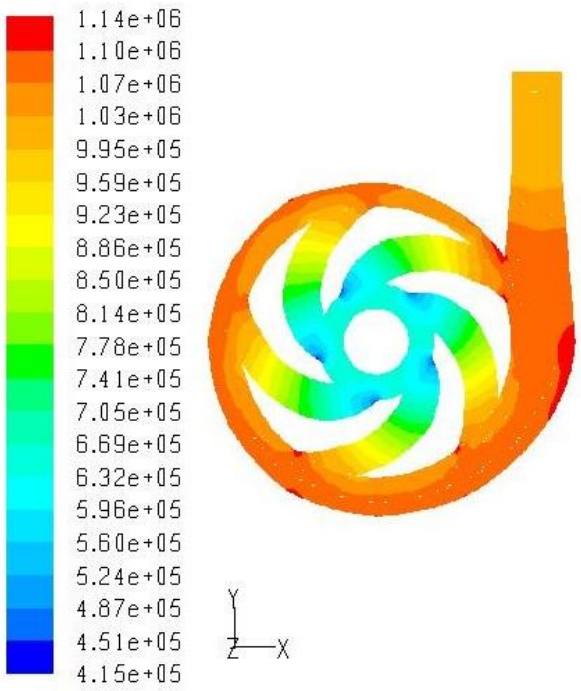

(c)

Figure 4.4: Contour of Static pressure (Pascal) at BEP for (a) Coal (b) lime stone (c) zinc tailings at 1450 rpm

After calculation, it is found that the efficiency is maximum in case of coal minerals at 9.73 lps flow rate for 50% concentration by weight and In case of limestone, efficiency is maximum at 15.36 lps flow rate for 40% concentration by weight and for the zinc tailings, efficiency is maximum at 15.07 lps flow rate for 55% concentration by weight. Figure 4.4 shows the static pressure contour (Pascal) for coal, limestone and zinc tailings at best efficiency point (BEP). Static pressure increases gradually from inlet to outlet of impeller. At the impeller suction side, pressure is low as compared to the pressure side.

The three curves are plotted between head and mass flow rate, input power and mass flow rate, efficiency and mass flow rate. These curves are basically known as the performance characteristics curve of the the pump.These curves are ploted for all three minerals. The performance characterstics curve of the the existing pump are given below :

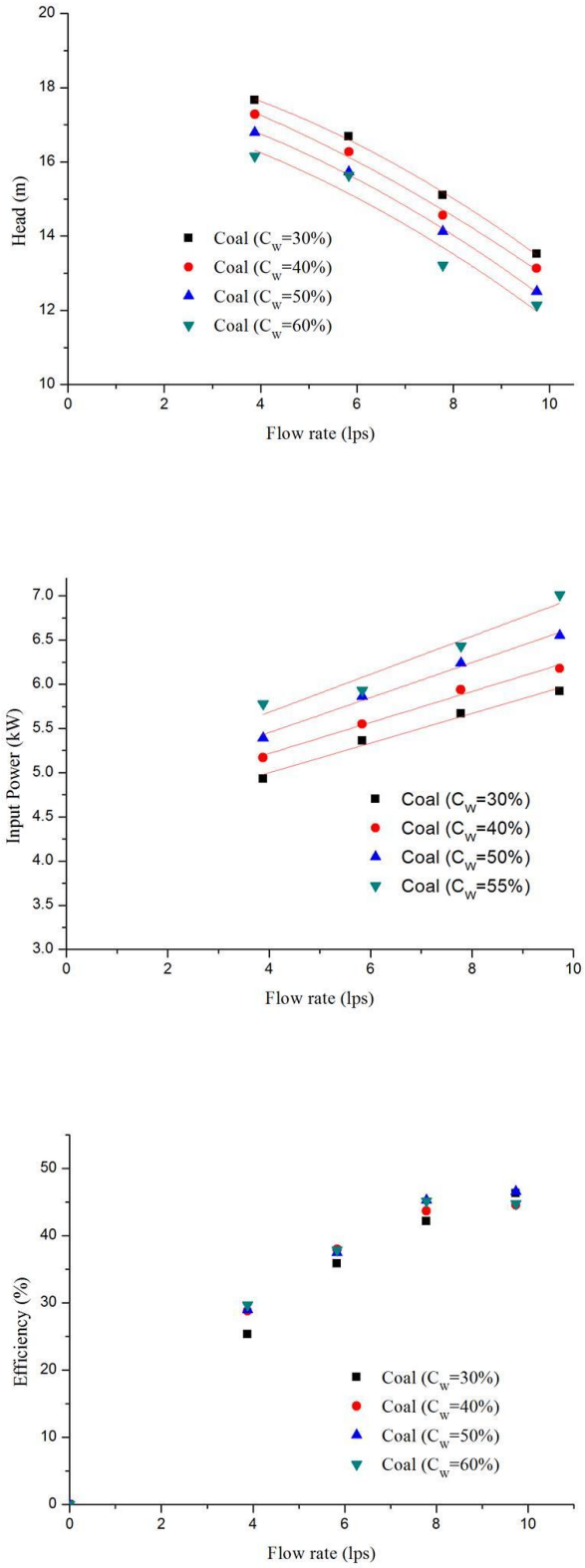

Figure 4.5: Performance of the pump with coal slurry at 1450 rpm

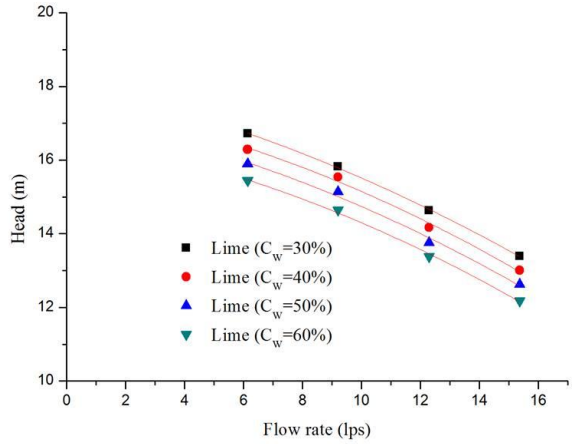

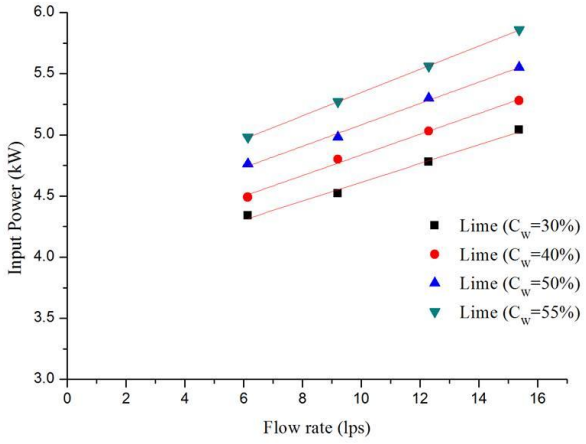

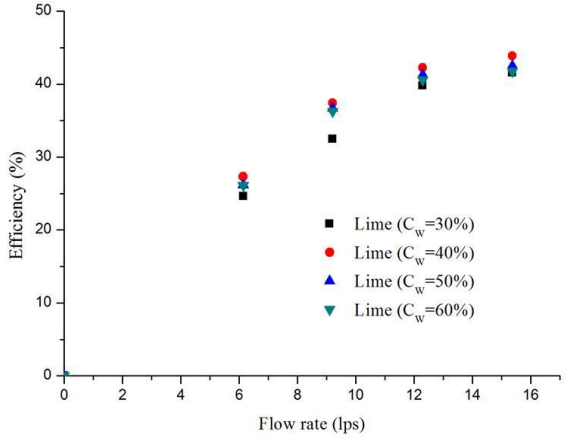

Figure 4.6: Performance of the pump with Lime Stone slurry at 1450 rpm

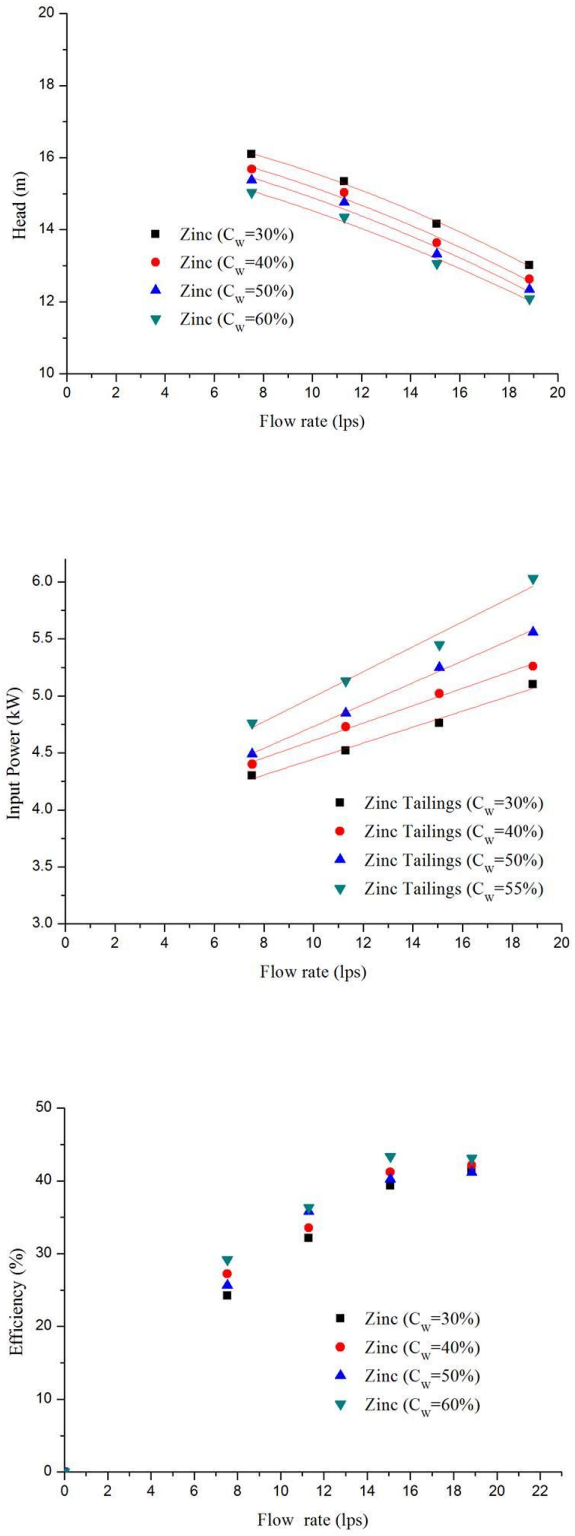

Figure 4.7: Performance of the pump with Zinc Tailings slurry at 1450 rpm

4.10 INFLUENCE OF PARTICLE DIAMETER ON THE FLOW FIELD

Figure 4.6 shows the distribution of coal volume fraction of the existing pump at 30 % concentration by weight, d = 0.031 mm and 0.175 mm. Figure 4.7 shows the distribution of coal volume fraction in the existing pump at 55 % concentration by weight , d = 0.031mm and 0.175 mm. Here simulation is conducted at different two concentrations by varying the diameter of the particles at same mass flow rate 3.88 lps. Due to effect of centrifugal and inertial force, particles start to flow along the pressure surface of the impeller and particles mainly accumulate near the exit region of the volute. At the tongue region, the largest volume fraction of coal is observed. At the entering portion of volute, some particle can flow out directly and exit the volute after circling the several times around the volute but a larger number of particles collide with the wall of volute.

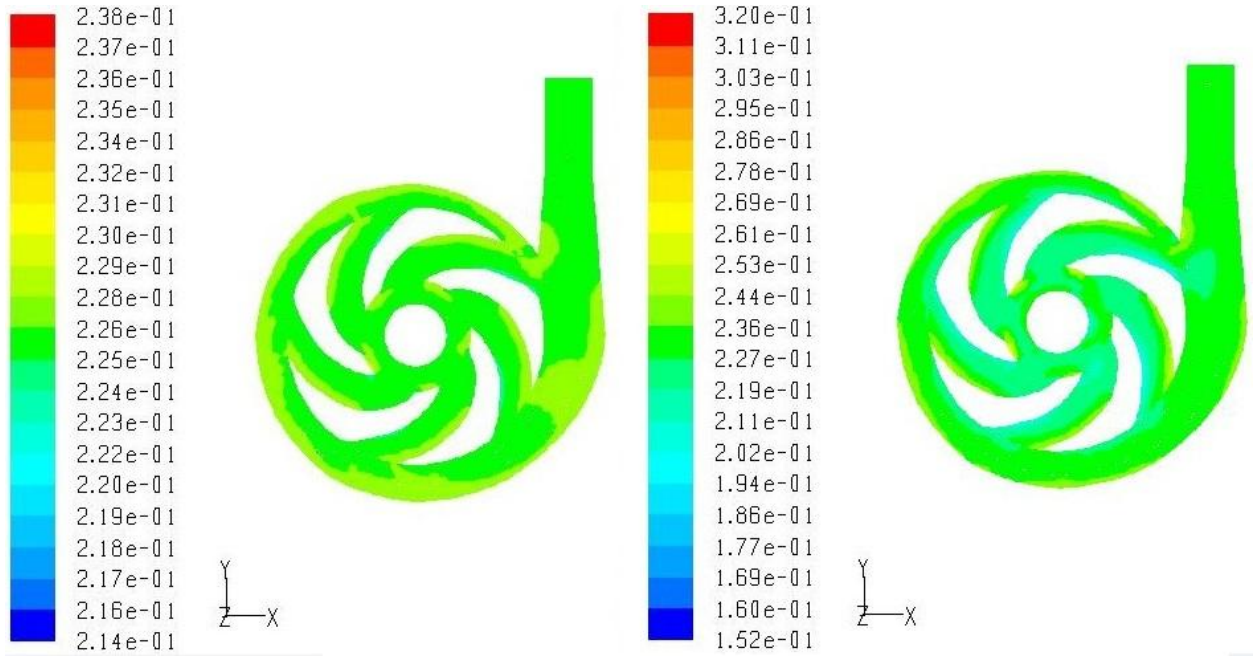

(a) d = 0.031 mm **(b) d = 0.175 mm**

Figure 4.8: Coal volume fraction contour at the condition of 30% Concentration

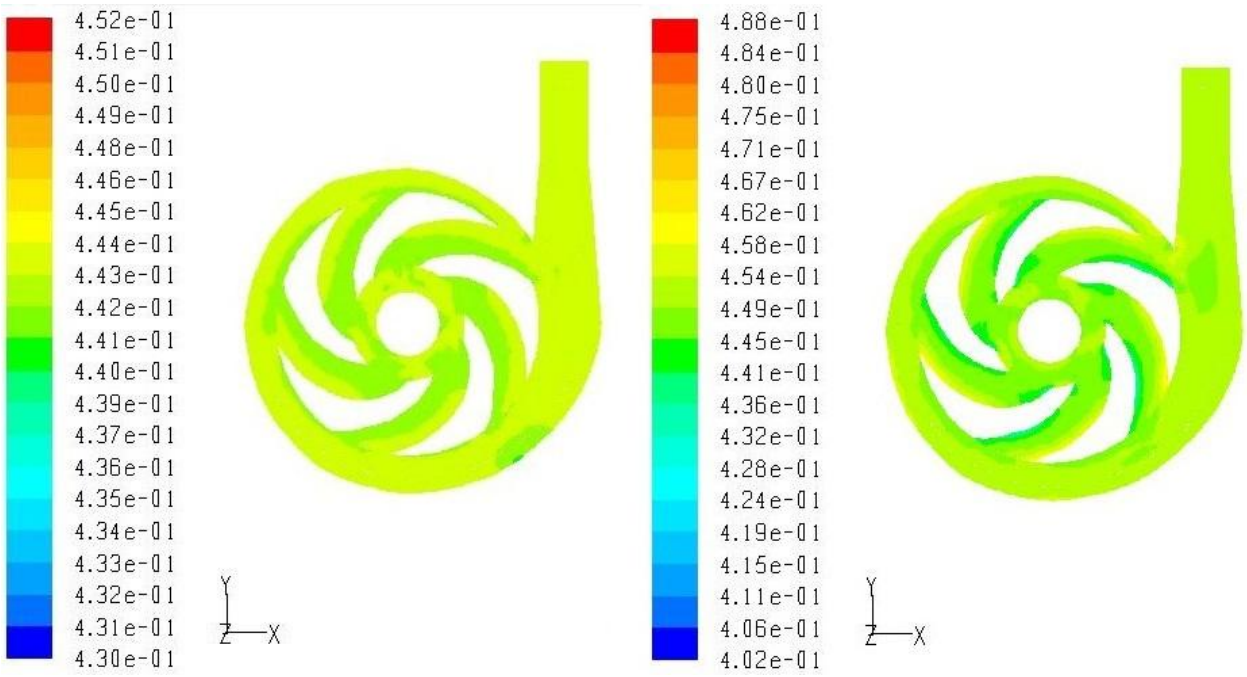

(a) d = 0.031 mm **(b) d = 0.175 mm**

Figure 4.9: Coal volume fraction contour at the condition of 55% Concentration

It is found that the diameter of particle has great effect on the distribution of coal volume fraction. Due to increase in the particle diameter, particles try to accumulate on the pressure side and pressure side of the blade is crased by the maximum particles.

4.11 INFLUENCE OF COAL, LIMESTONE AND ZINC TAILNGS VOLUME FRACTION ON THE FLOW FIELD

Figure 4.8 shows the distribution of coal volume fraction of the existing pump at 3.88 lps, d=0.031mm, C_w = 30%, 40%, 50% and 55%. Figure 4.9 shows the distribution of coal volume fraction of the existing pump at 9.73 lps, d=0.031mm, C_w = 30%, 40%, 50% and 55 %.

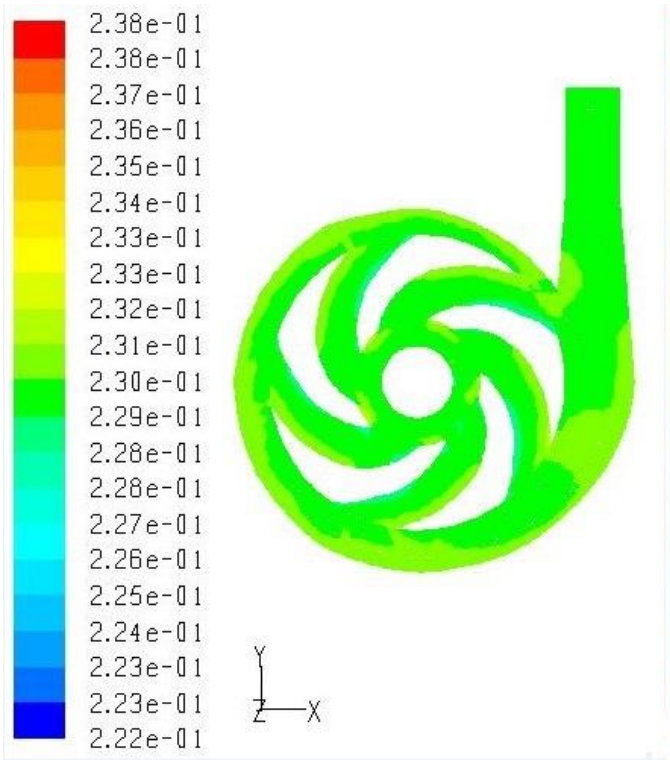

(a) Concentration = 30%

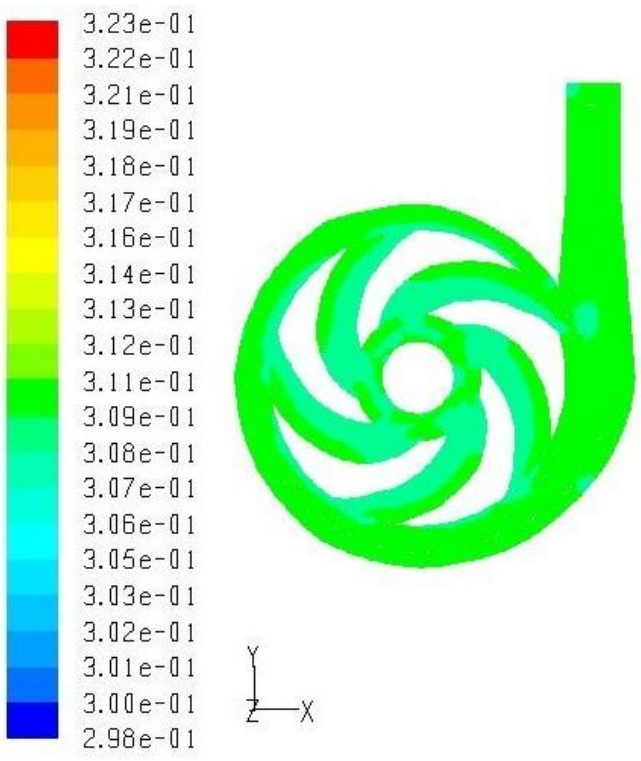

(b) Concentration = 40%

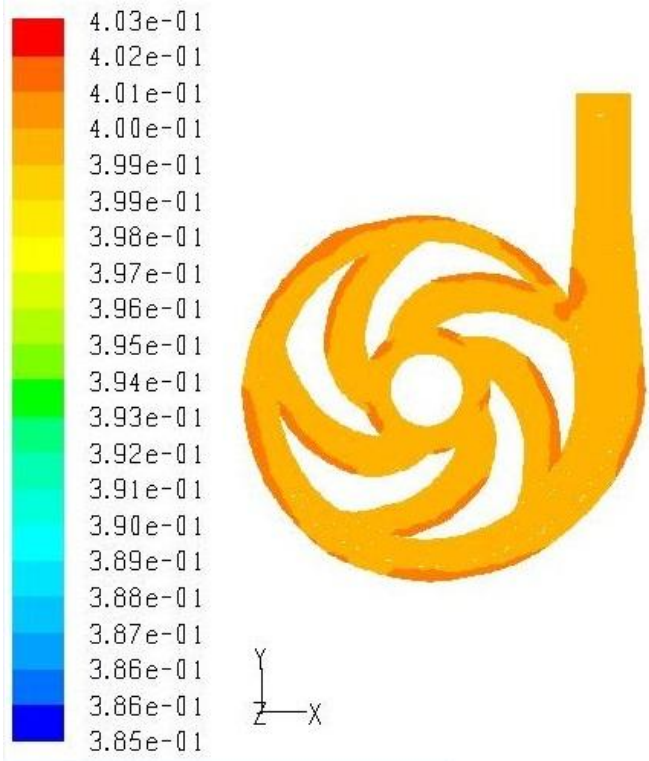

(c) Concentration = 50%

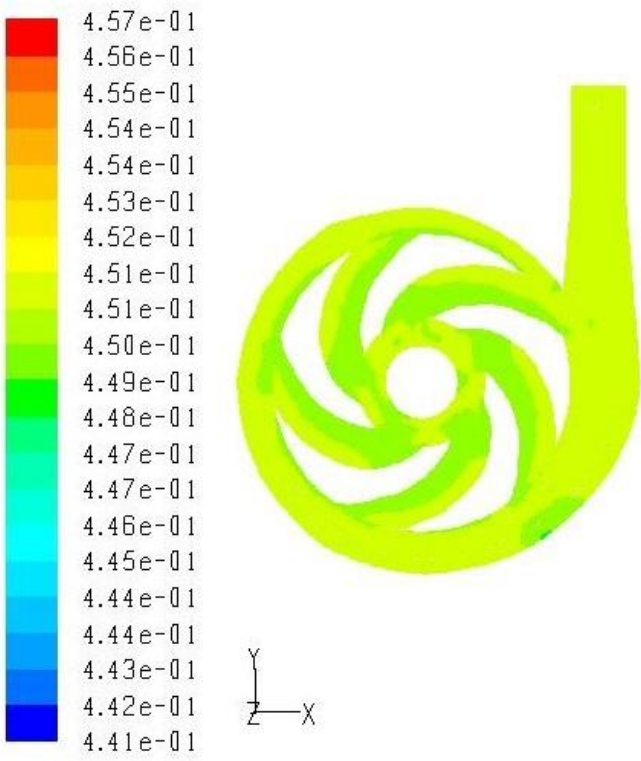

(d) Concentration = 55%

Figure 4.10: Coal volume fraction contour at the condition of 3.8 lps, d= 0.031mm

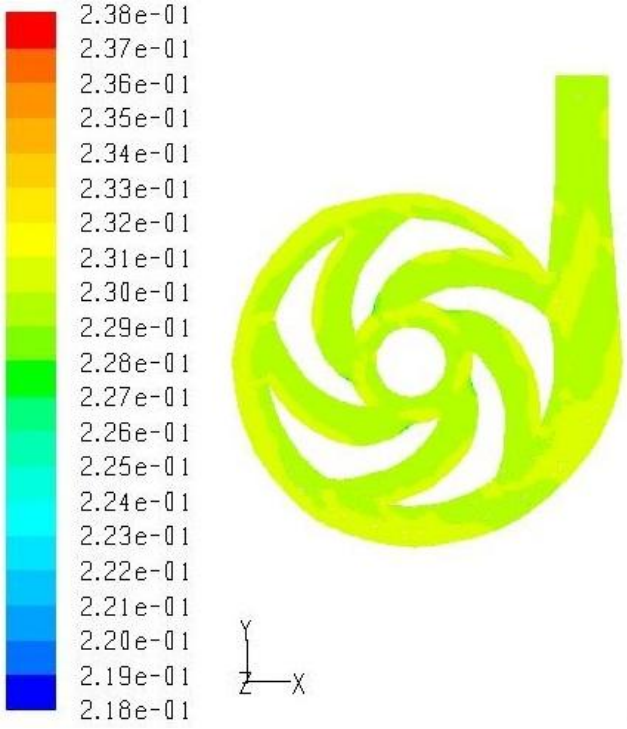

(a) Concentration = 30%

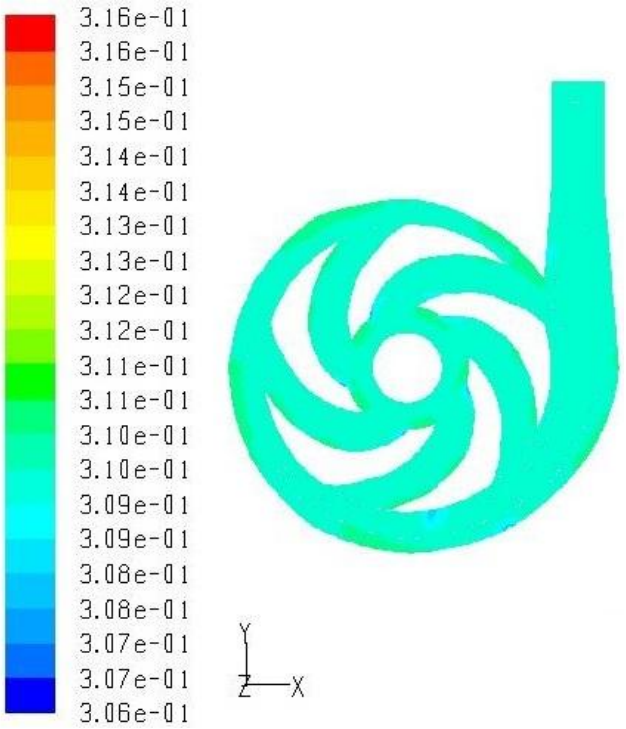

(b) Concentration = 40%

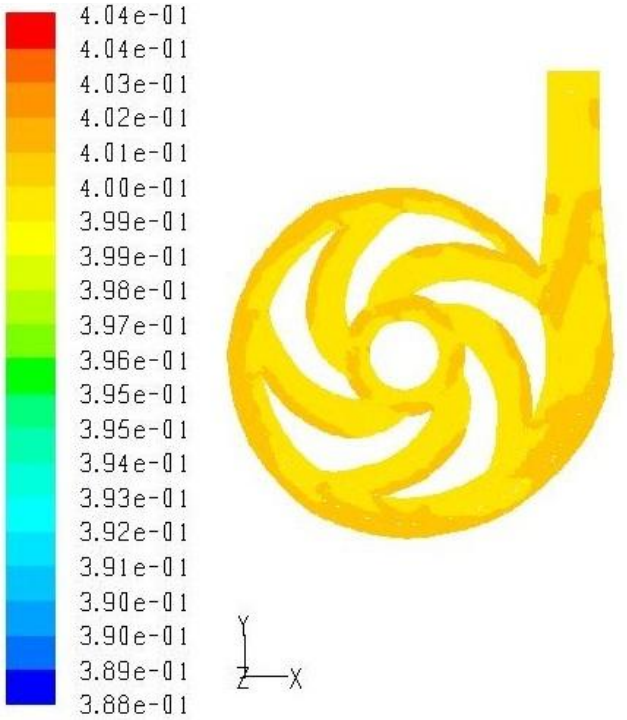

(c) Concentration = 50%

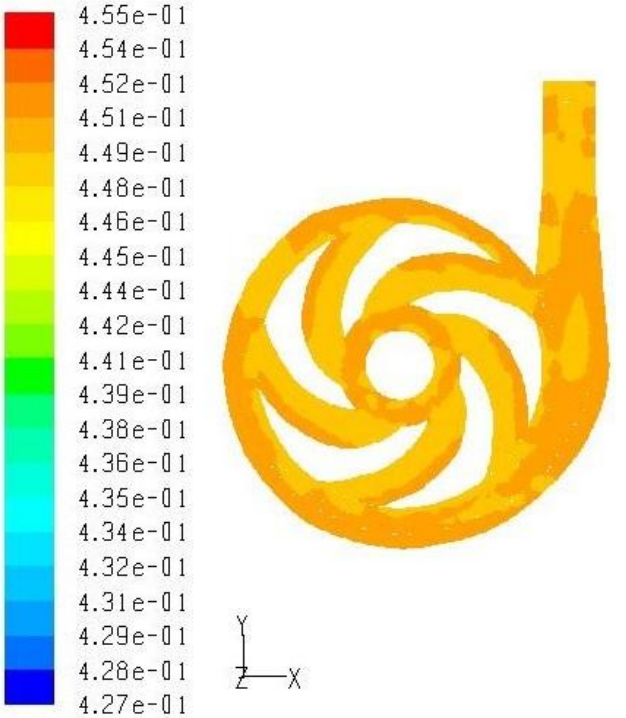

(d) Concentration = 55%

Figure 4.11: Coal volume fraction contour at the condition of 9.7 lps, d= 0.031mm

Due to increase in the flow rate, volume fraction of coal of the existing pump is smaller than the small flow rate. The effect of the volume fraction on the gratitude of the coal volume fraction is less than the diameter of the particle in the existing pump.

Figure 4.10 shows the distribution of limestone volume fraction of the existing pump at 6.14 lps, d=0.031mm, C_w = 30%, 40%, 50% and 55%. Figure 4.11 shows the distribution of limestone volume fraction of the existing pump at 15.36 lps, d=0.031mm, C_w = 30%, 40%, 50% and 55 %.

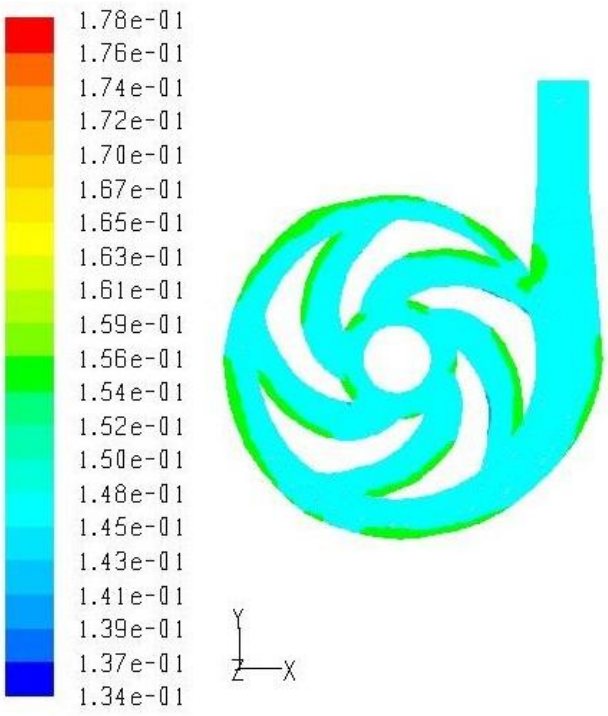

(a) Concentration = 30%

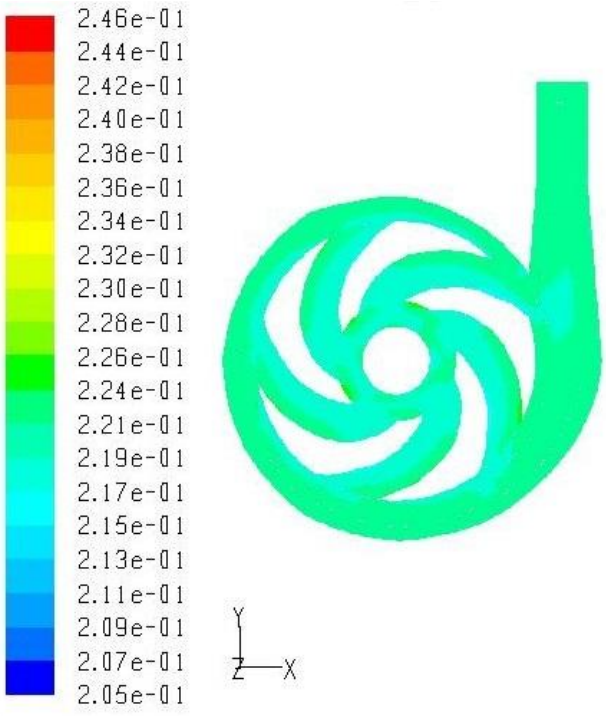

(b) Concentration = 40%

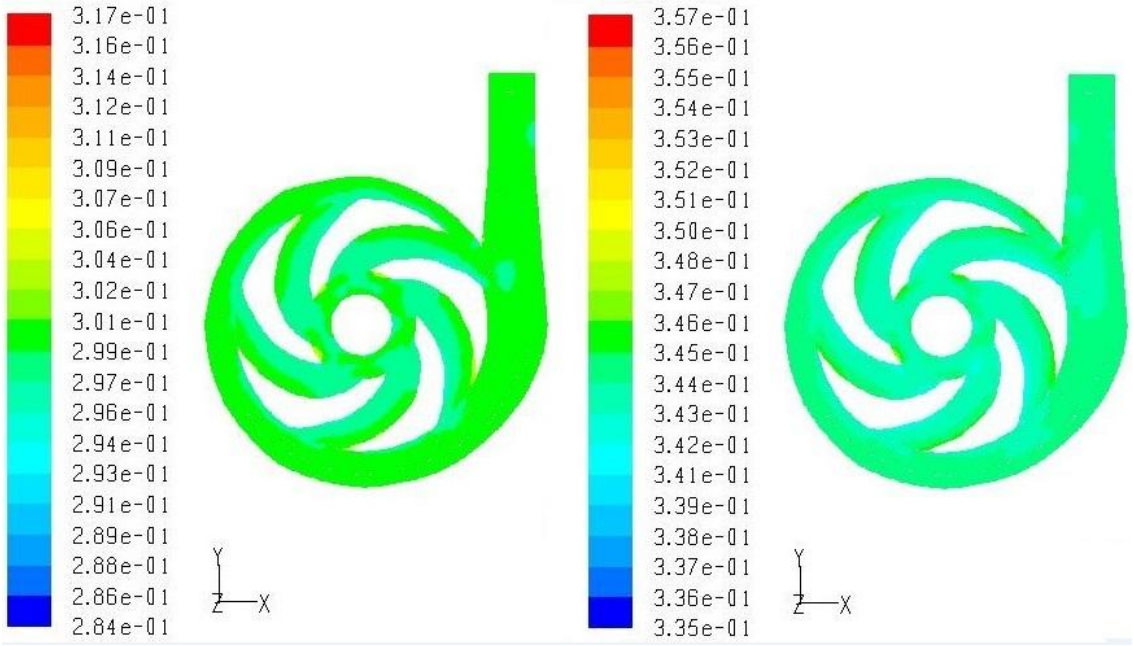

(c) Concentration = 50% **(d) Concentration = 55%**

Figure 4.12: Limestone volume fraction contour at the condition of 6.14 lps, d= 0.033mm

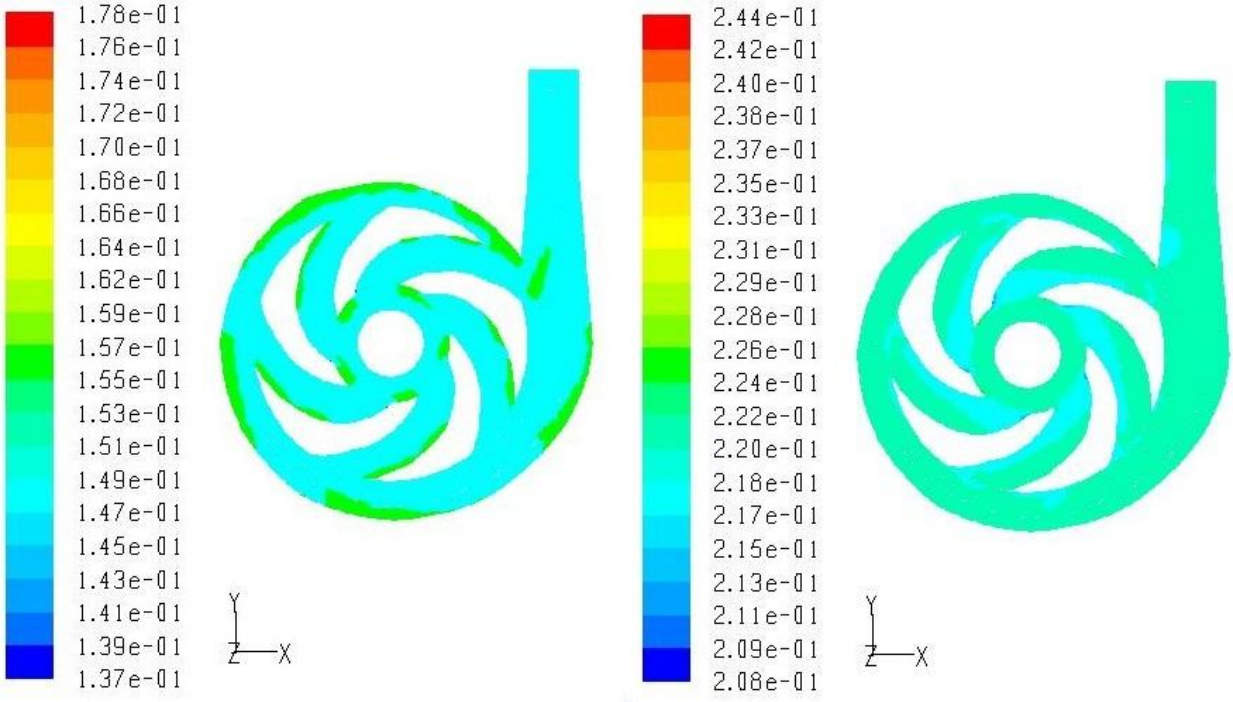

(a) Concentration = 30% **(b) Concentration = 40%**

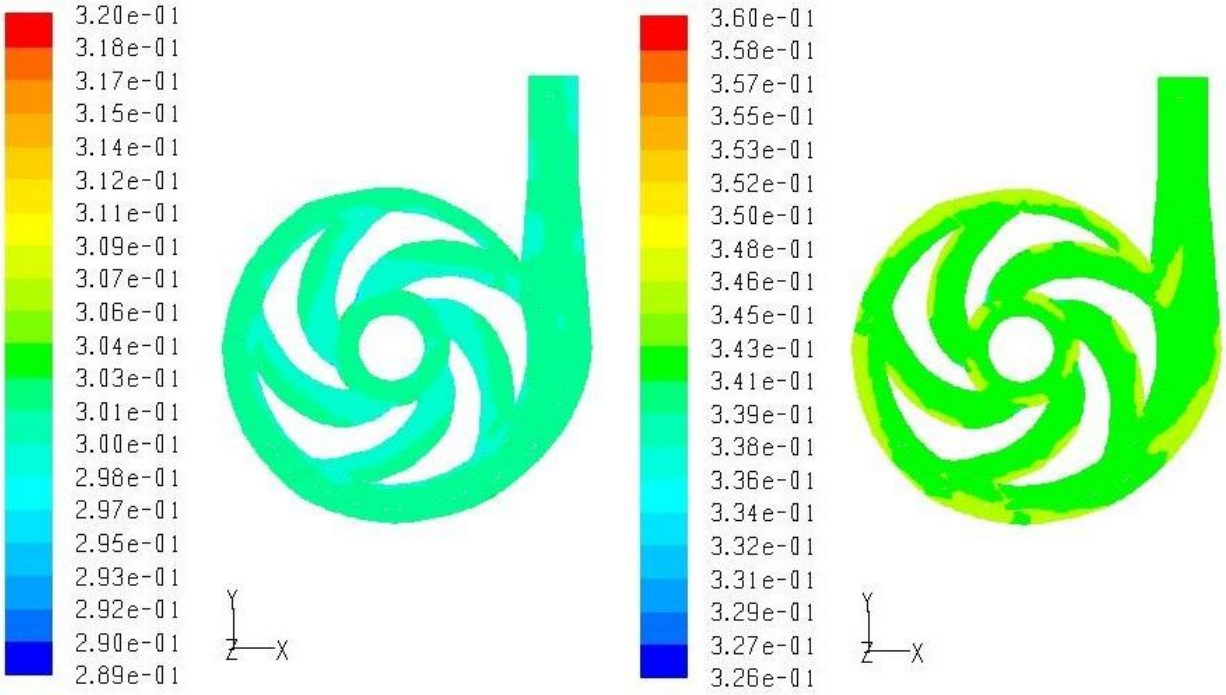

(c) Concentration = 50% **(d) Concentration = 55%**

Figure 4.13: Limestone volume fraction contour at the condition of 15.36 lps, d= 0.033mm

The effect of volume fraction is less than effect of the particle diameter. At 6.14 lps flow rate limestone volume fraction is greater than the 15.36 lps flow rate. Due to increase in the density of the solid material, volume fraction decreases. The volume fraction of limestone is small as compared to the coal because the density of coal is smaller than the density of the limestone.

And due to increase in the flow rate, volume fraction of limestone of the exiting pump is smaller than the small flow rate.

Figure 4.12 shows the distribution of zinc tailings volume fraction the existing pump at 7.53 lps, d=0.031mm, C_w = 30%, 40%, 50% and 55%. Figure 4.13 shows the distribution of zinc tailings volume fraction the existing pump at 18.83 lps, d=0.031mm, C_w = 30%, 40%, 50% and 55 %.

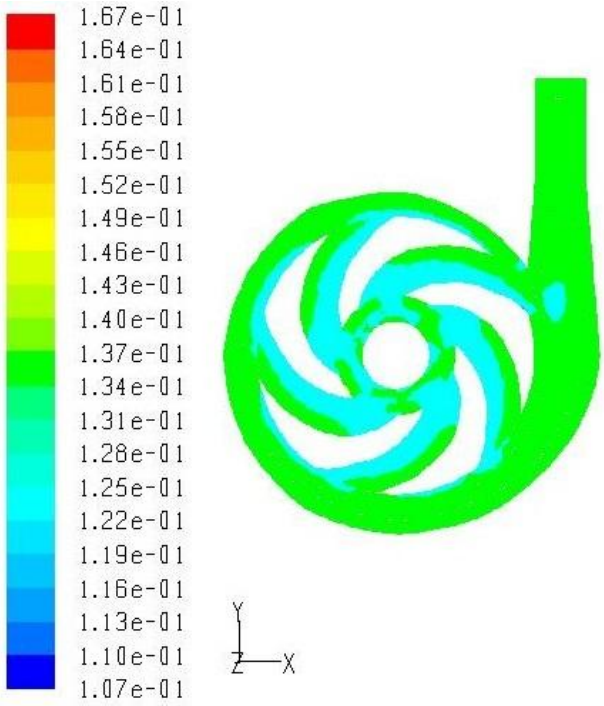

(a) Concentration = 30%

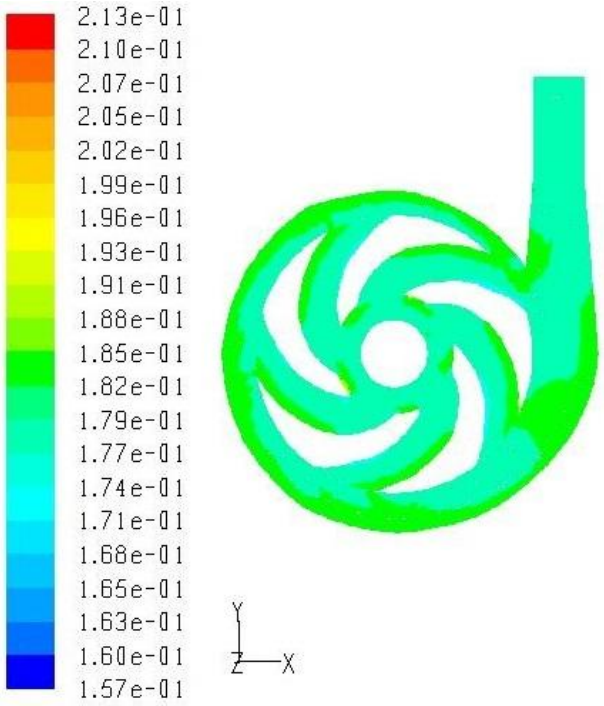

(b) Concentration = 40%

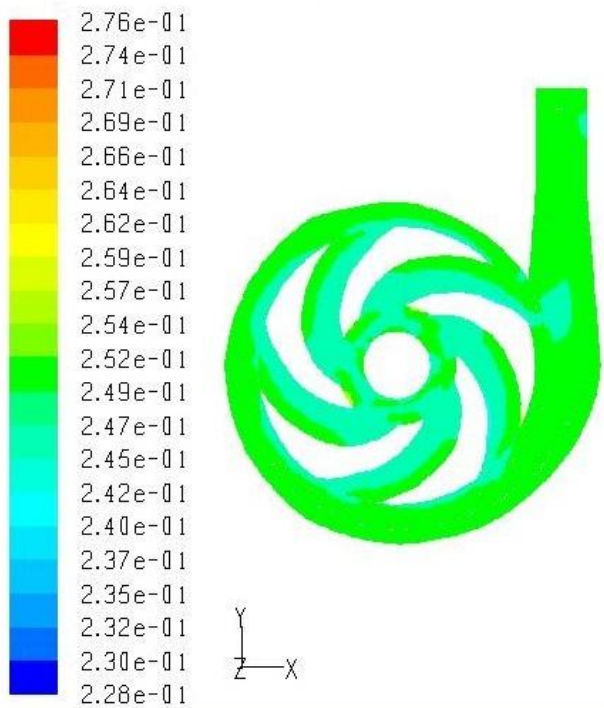

(c) Concentration = 50%

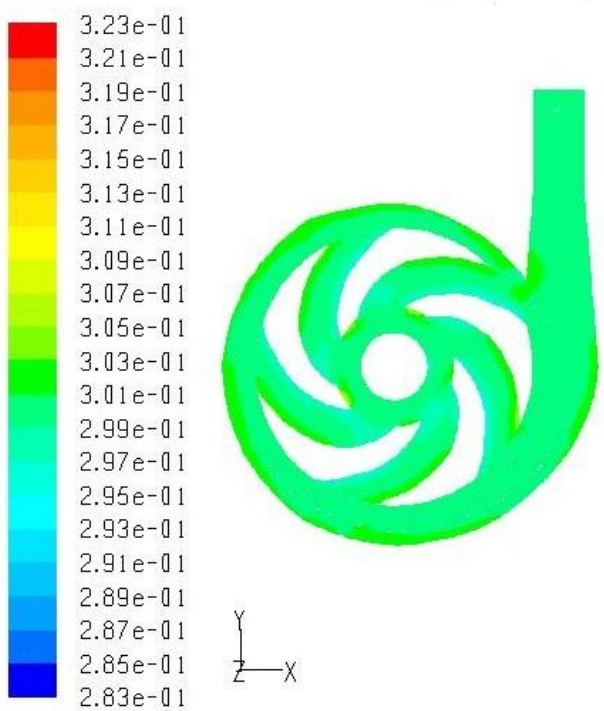

(d) Concentration = 55%

Figure 4.14: Zinc volume fraction contour at the condition of 7.53 lps, d= 0.033mm

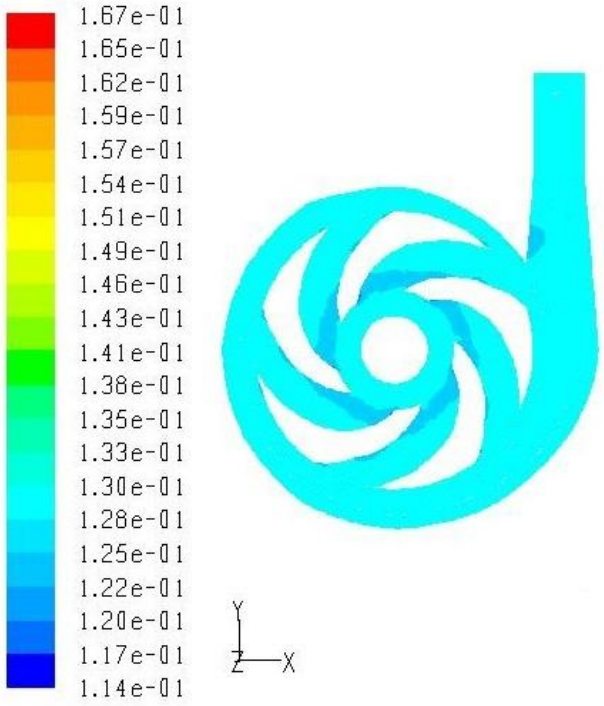

(a) Concentration = 30%

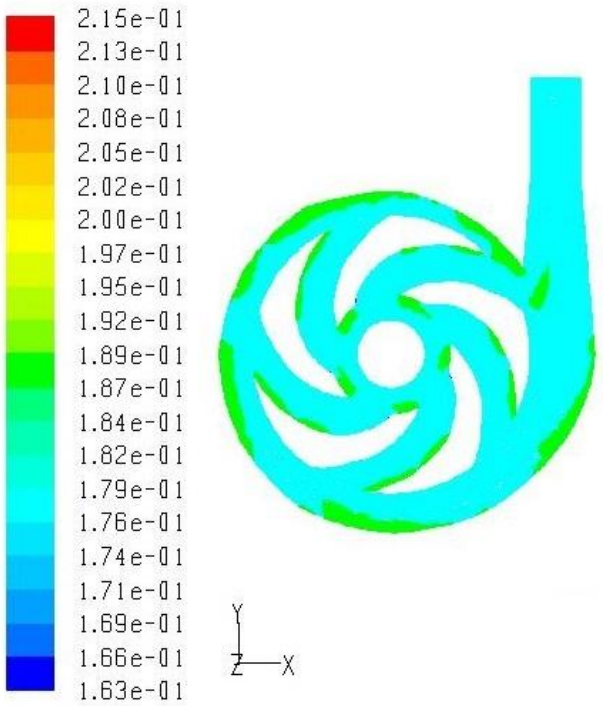

(b) Concentration = 40%

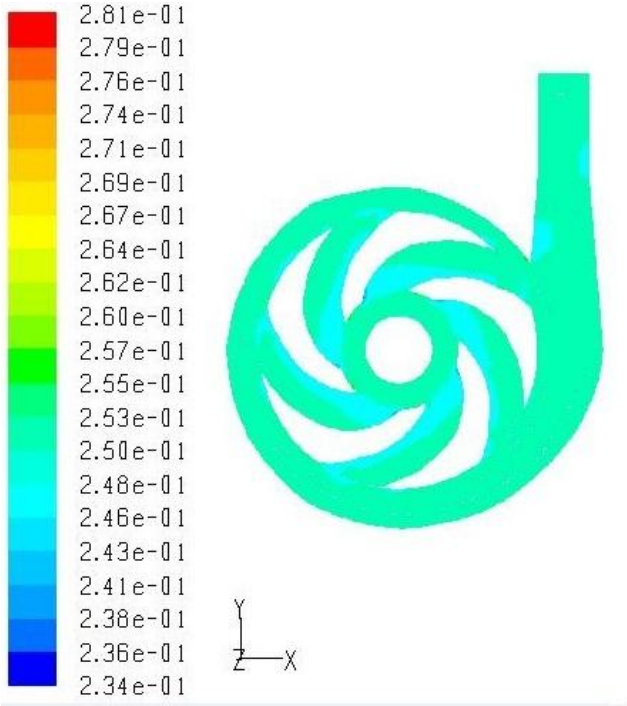

(c) Concentration = 50%

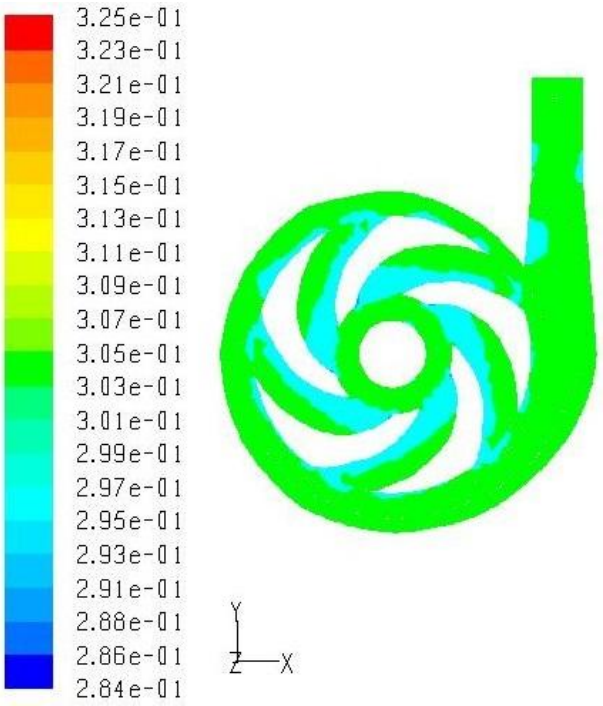

(d) Concentration = 55%

Figure 4.15: Zinc volume fraction contour at the condition of 18.83 lps, d= 0.033mm

At 7.53 lps flow rate zinc tailings volume fraction is greater than the 18.83 lps flow rate. Due to increase in the density of the solid material, volume fraction decreases. The volume fraction of zinc tailings is small as compared to the limestone and coal because the density of limestone and coal is smaller than zinc tailings density. And zinc tailings volume fraction at 18.83 lps flow rate of the exiting pump is smaller than the 7.53 lps flow rate.

4.12 DESIGN MODIFICATION IN CENTRIFUGAL SLURRY PUMP

The existing design of pump is analyzed for some modification in the design. Although the pump is working well in single phase and two phase both. To make the design improvements first of all the results and contours of computational analysis is thoroughly studied and then new design is suggested in the existing pump with changing in the impeller design of the pump. The impeller is changing by variation in number of blade. The effect of different blade numbers on the pump performance will study in next chapter.

CHAPTER 5

SIMULATION OF PUMP PERFORMANCE WITH VARIATION IN BLADE NUMBER

In the present chapter the modeling of impeller with different blade number (4, 5, 6, 7 and 8) is discussed and the computational results obtained with different impeller and compared with the original design having number of blade 5.

The effect of different blade numbers on the pump performance has been studied in this chapter by taking comparisons data of blade number: 4, 5, 6, 7 and 8. The performance of pump is evaluated with water at two different speed 1450 rpm and 1750 rpm.

5.1 MODELING OF PUMP WITH DIFFERENT BLADE NUMBER

All the parts of the existing pump remain same for the models with 4, 5, 6, 7 and 8 blades, only impeller is different.

Impeller

The existing centrifugal pump contains the impeller with 5 number of blade and is of enclosed type. Impeller with 4, 6, 7 and 8 blade is modeled using the principle blade design of the existing pump with GAMBIT software. Impeller with different blade numbers is shown in Figure 6.1.

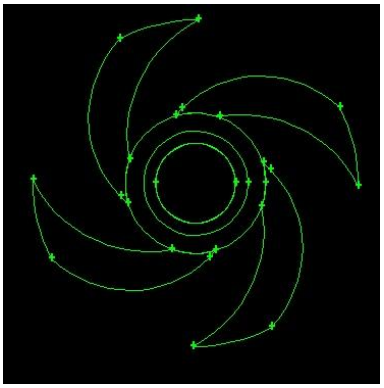

(a)

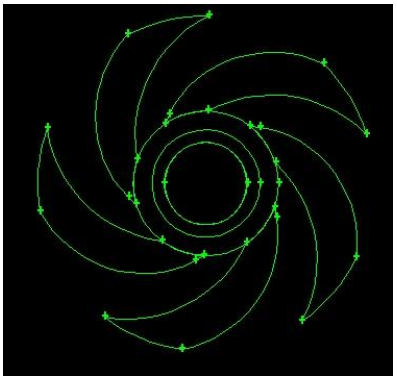

(b)

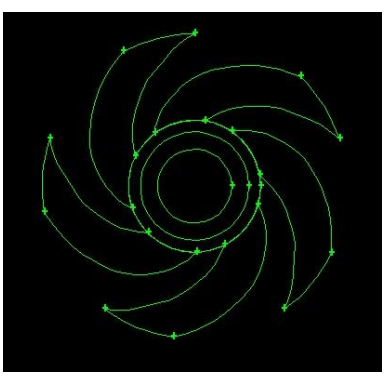

(c)

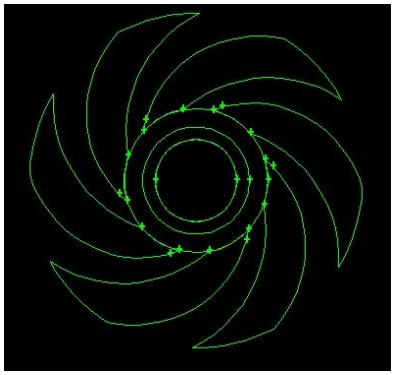

(d)

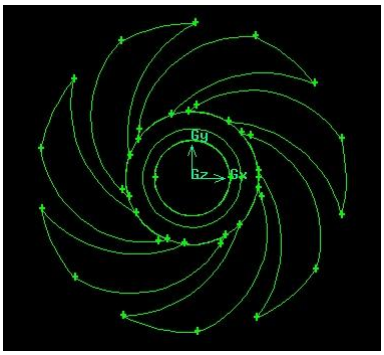

(e)

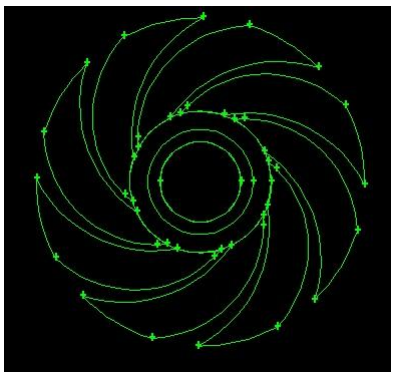

(f)

Figure 5.1: Impeller design with (a) 4 blade (b) 5 blade (c) existing model with 5 blade(d) 6 blade (e) 7 blade (f) 8 blade

Other components of the pump are designed as same method which is explained in earlier chapter.

Meshing

The next step after modeling the pump component is to descretize it into smaller mesh elements. This process of discretization is called meshing. The meshing is done on the GAMBIT 2.3.16 package. Meshing can be done by using different type of elements such as tetrahedral, hexahedral, wedge etc. A tetrahedral-hex core meshing is done for all the component of the centrifugal slurry pump. Fine meshing is used for the region where the forces are more significant and coarser meshing size function is done for all other regions. It is important to check the quality of mesh, because parameter such as skewness affects the

accuracy of the CFD simulation. The quality of mesh is checked by calculating the equisize skewness, aspect ratio and equiangle skewness. Each element has of value of skewness between 0 and 1. All of the elements in mesh have positive area/volume otherwise the simulation in 'FLUENT' solver is not possible. After meshing file is saves as .msh and when this file is open in fluent software, a grid sensitivity test is done for the models with different number of blades. A finer meshing scheme is used to take in consideration of the every vital fact which is affecting the flow in case of single as well as multi-phase flow.

5.2 PRESSURE DISTRIBUTION WITH VARIATION IN BLADE NUMBER

Single phase Simulation has been applied with the models of the pump with 4, 5, 6, 7 and 8 blade at 1450 rpm and 1750 rpm and 2.64 lps flow rates. Figure 5.2 shows the static pressure contours with water at 1450 rpm and 2.64 lps for all number of blades.

From the figure 5.2 it is clear that the 4 blade design is generating less head as compared to the other models with blade number 5, 6, 7 and 8. Due to increase in the blade number, the value of static pressure also increases. Figure 5.3 shows that the static pressure contour (Pascal) at 1750 rpm. We can see that as the rotational speed increases, the value of maximum pressure also increases. Therefore rotational speed and number of blade have a significant effect on centrifugal pumps. Rotational speed and static pressure play an important role for calculating the head as well as the total efficiency. The performance of the pump at 1450 rpm and 1750 rpm is given in Table 5.1.

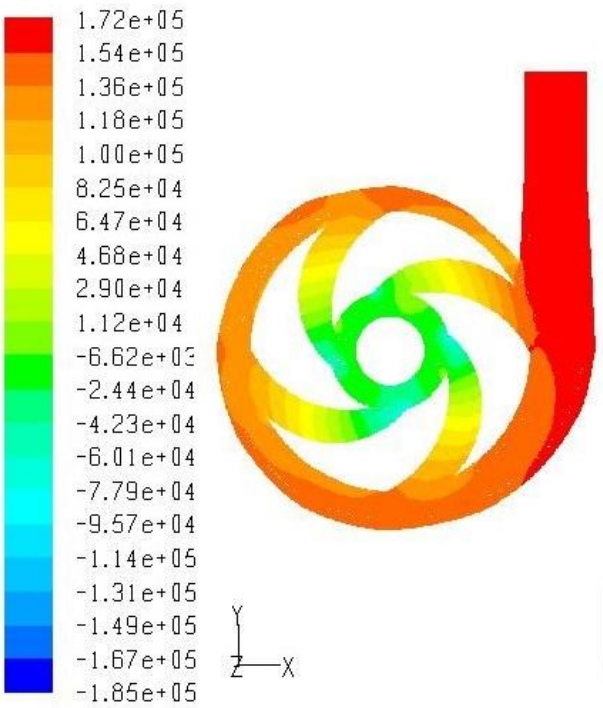
1.72e+05
1.54e+05
1.36e+05
1.18e+05
1.00e+05
8.25e+04
6.47e+04
4.68e+04
2.90e+04
1.12e+04
-6.62e+03
-2.44e+04
-4.23e+04
-6.01e+04
-7.79e+04
-9.57e+04
-1.14e+05
-1.31e+05
-1.49e+05
-1.67e+05
-1.85e+05
Y
Z
X

(a)

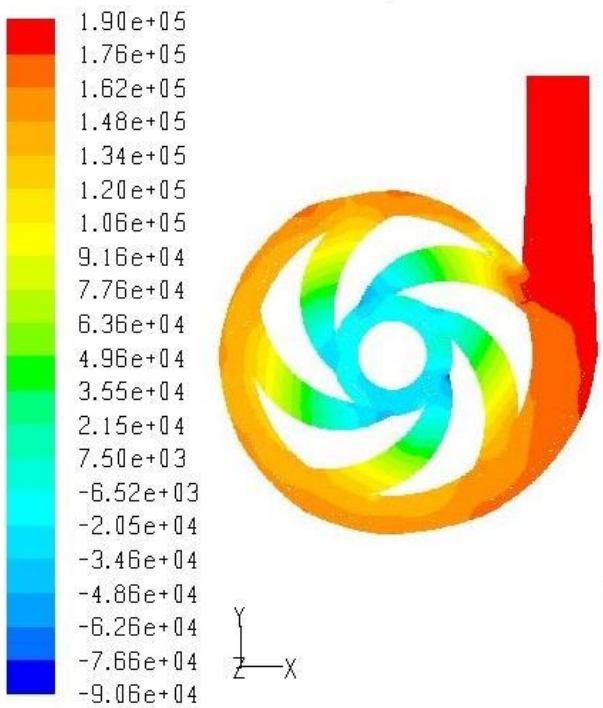
1.90e+05
1.76e+05
1.62e+05
1.48e+05
1.34e+05
1.20e+05
1.06e+05
9.16e+04
7.76e+04
6.36e+04
4.96e+04
3.55e+04
2.15e+04
7.50e+03
-6.52e+03
-2.05e+04
-3.46e+04
-4.86e+04
-6.26e+04
-7.66e+04
-9.06e+04
Y
Z
X

(b)

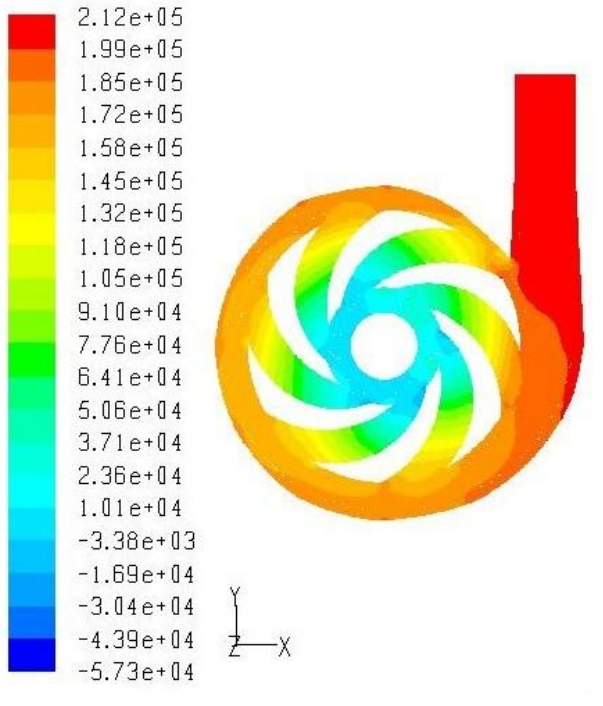
2.12e+05
1.99e+05
1.85e+05
1.72e+05
1.58e+05
1.45e+05
1.32e+05
1.18e+05
1.05e+05
9.10e+04
7.76e+04
6.41e+04
5.06e+04
3.71e+04
2.36e+04
1.01e+04
-3.38e+03
-1.69e+04
-3.04e+04
-4.39e+04
-5.73e+04
Y
Z
X

(c)

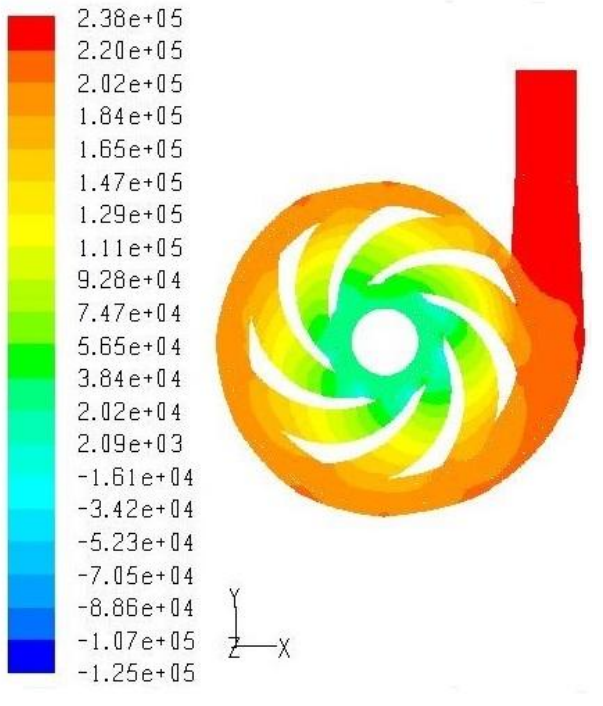
2.38e+05
2.20e+05
2.02e+05
1.84e+05
1.65e+05
1.47e+05
1.29e+05
1.11e+05
9.28e+04
7.47e+04
5.65e+04
3.84e+04
2.02e+04
2.09e+03
-1.61e+04
-3.42e+04
-5.23e+04
-7.05e+04
-8.86e+04
-1.07e+05
-1.25e+05
Y
Z
X

(d)

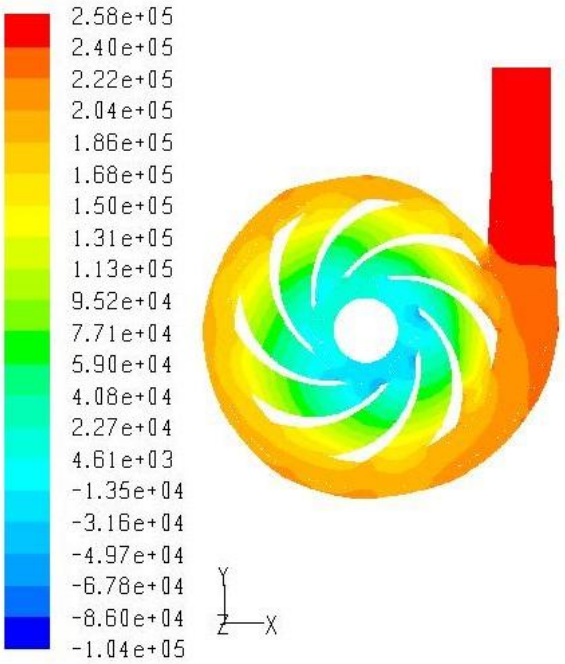

(e)

Figure 5.2: Contour of Static pressure (Pascal) for (a) 4 blade (b) 5 blade (c) 6 blade (d) 7 blade (e) 8 blade at 1450 rpm and 2.64 lps with water

Table 5.1 Performance of the pump at 1450rpm and 1750 rpm

	Head(m) at 1450 rpm and 2.64 lps	**Head(m) at 1750 rpm and 2.64 lps**
4 blade	15.53	20.29
5 blade	17.94	25.73
6 blade	19.62	27.16
7 blade	20.90	28.25
8 blade	21.76	29.32

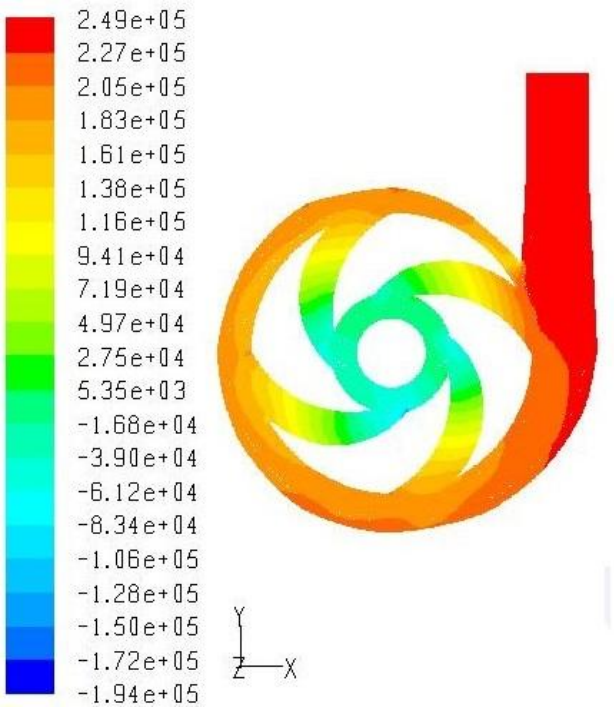
2.49e+05
2.27e+05
2.05e+05
1.83e+05
1.61e+05
1.38e+05
1.16e+05
9.41e+04
7.19e+04
4.97e+04
2.75e+04
5.35e+03
-1.68e+04
-3.90e+04
-6.12e+04
-8.34e+04
-1.06e+05
-1.28e+05
-1.50e+05
-1.72e+05
-1.94e+05
Y
Z
X

(a)

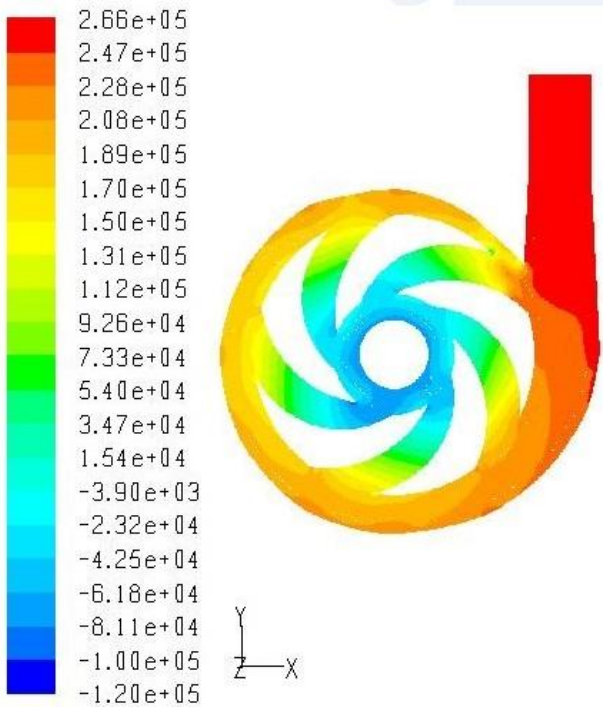
2.66e+05
2.47e+05
2.28e+05
2.08e+05
1.89e+05
1.70e+05
1.50e+05
1.31e+05
1.12e+05
9.26e+04
7.33e+04
5.40e+04
3.47e+04
1.54e+04
-3.90e+03
-2.32e+04
-4.25e+04
-6.18e+04
-8.11e+04
-1.00e+05
-1.20e+05
Y
Z
X

(b)

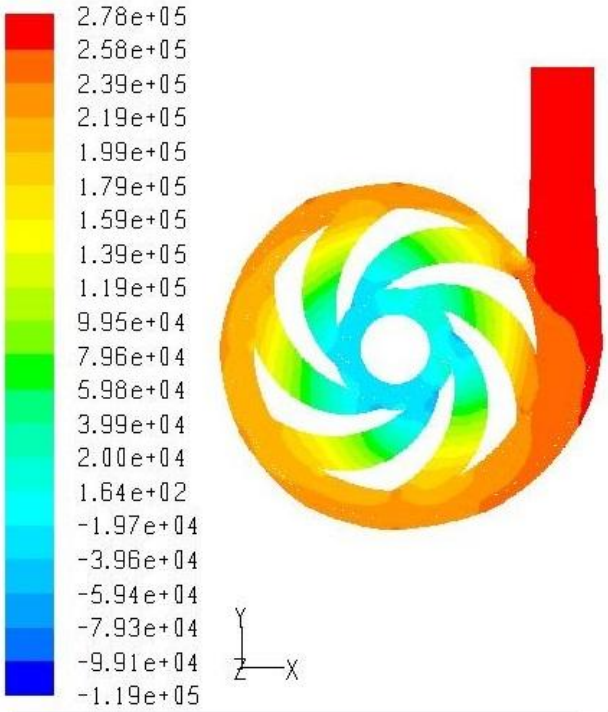
2.78e+05
2.58e+05
2.39e+05
2.19e+05
1.99e+05
1.79e+05
1.59e+05
1.39e+05
1.19e+05
9.95e+04
7.96e+04
5.98e+04
3.99e+04
2.00e+04
1.64e+02
-1.97e+04
-3.96e+04
-5.94e+04
-7.93e+04
-9.91e+04
-1.19e+05
Y
Z
X

(c)

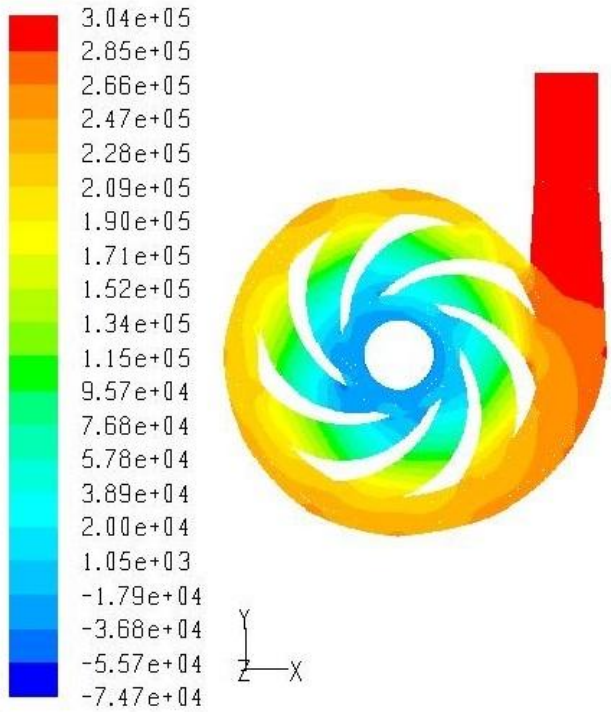
3.04e+05
2.85e+05
2.66e+05
2.47e+05
2.28e+05
2.09e+05
1.90e+05
1.71e+05
1.52e+05
1.34e+05
1.15e+05
9.57e+04
7.68e+04
5.78e+04
3.89e+04
2.00e+04
1.05e+03
-1.79e+04
-3.68e+04
-5.57e+04
-7.47e+04
Y
Z
X

(d)

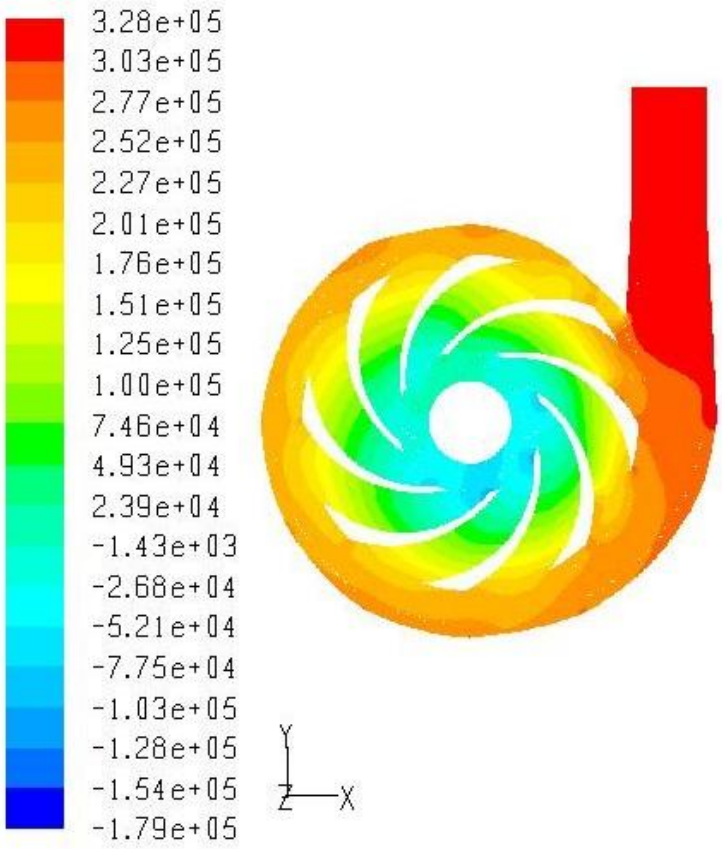

(e)

Figure 5.3: Contour of Static pressure (Pascal) for (a) 4 blade (b) 5 blade (c) 6 blade (d) 7 blade (e) 8 blade at 1750 rpm and 2.64 lps with water

The 4 blade model developed less head as compared to other. The maximum head is developed by the 8 blade model. It is cleared that due to increase in the blade number and the rotational speed, the pump head increases. More head is developed at 1750 rpm than the 1450 rpm. So it is cleared that the centrifugal pump head increases due to increase in rotational speed. At suction side of the blade inlet of the impellers with different blade number all have an obvious low pressure area. The area flow pressure region grows continuously with the increase of the blade number.

CHAPTER 6

CONCLUSION AND FUTURE SCOPE

6.1 CONCLUSION

CFD simulations have been conducted to investigate the solid-liquid two-phase flow in centrifugal pump at both small flow rate and large flow rate conditions. The static pressure contour of coal and volume fraction contour of coal, limestone and zinc tailings are quantitatively examined in details. Pump performance studied with variation of number of blades at speed 1450 and 1750 rpm. At the same particle size, the pump head decreases and shaft power increases with the increase of particle concentration. Particle diameter has great influence on the distribution of the coal volume fraction. The effect of the particle diameter is more than the effect of volume fraction .As the particle diameter increases, particles try to accumulate on the pressure side. When the density of the solid material increases, volume fraction decreases. The volume fraction of zinc tailings is small as compared to the limestone and coal because the density of limestone and coal is smaller than zinc tailings density. Head of the pump increases with increase the number of blade and rotational speed. There is a low pressure area at the suction side of the blade inlet of the impeller and it grows continuously with increase in number of blade.

6.2 FUTURE SCOPE

There is no doubt that a major focus of CFD is to enhance the design process for any machine that deals with fluid flow. Lots of parameters are present in order to improve the design of the centrifugal slurry pump:

- The geometrical parameters such as, blade angle, blade width, impeller diameter can be considered as further analysis.
- Changing in the Cutwater area of volute casing
- Modification in Tongue region

References

[1] https://www.google.co.in/search?q=centrifugal+pump&biw=

[2] Impeller of pump available on http://www.jensenengineeredsystems.com/impellers/

[3] https://www.google.co.in/search?q=vortex+casing+pump&tbm

[4] Wilcox David C, (1994), Turbulence Modeling For CFD, DCW Industries, Inc. La Canada, California, Second Edition, pp. 1-477.

[5] Versteeg H.K, Malalaasekera W, (1995), An introduction to computational fluid dynamics , the finite volume method, Longman Scientific & Technical, First Edition, pp. 1-267.

[6] Anderson John D., (1995), Computational Fluid Dynamics, The Basics With Applications, McGraw- Hill, Inc., Second Edition, pp. 1-563.

[7] Baha E. Abulnaga, (2002), Slurry Systems Handbook, McGraw-Hill Companies, USA, pp. 1-532.

[8] Chung T.J., (2002), Computational Fluid Dynamics, Cambridge University Press, First Edition, pp. 1-426.

[9] Wilson K.C., Addie G.R., Sellgren A. and Clift R., (2006), Slurry Transport Using Centrifugal Pumps, Springer Publication, Third Edition, pp. 1-441.

[10] Spence R, (2006), CFD Analysis of Centrifugal Pumps with Emphasis on Factors Affecting Internal Pressure Pulsations, PhD Thesis of Cranfield University School of Mechanical Engineering, pp. 1-380.

[11] Tu Jiyuan, Yeoh Guan Heng and Liu Chaogun, (2008), Computational Fluid Dynamics, A Practical Approach, Elesevier Publication, First Edition, pp. 1-469

[12] Luo Xianwu, Zhang Yao, Peng Junqi, Xu Hongyuan and Yu Weiping, (2008), Impeller Inlet Geometry Effect on Performace Improvement for Centrifugal Pumps, Journal of Mechanical Science And Technology, Vol. 22, pp. 1971-1976.

[13] Minggao Tan, Shouqi Yuan, Houlin Liu, Yong Wang and Kai Wang, (2009), Numerical Research on Performance Prediction for Centrifugal Pumps, Chinese Journal of Mechanical Engineering, Vol. 23, pp. 1-6.

[14] Karanth k. Vasudeva and Sharma N. Yagnesh, (2009), Numerical Analysis on The Effect of Varying Number of Diffuser Vanes on Impeller-Diffuser Flow Interaction in a Centrifugal Fan, World Journal of Modeling And Simulation, Vol. 5, pp. 63-71.

[15] Bacharoudis E.C., Filios A.E., Mentoz M.D. and Margaris D.P., (2009), Parametric study of a Centrifugal Pump Impeller by Varying the Outlet Blade Angle, The Open Mechancial Engineering Journal, Vol. 2, pp. 75-83.

[16] Ozturk Adnan, Aydin Kadir, Sahin Besir and Pinarbasi Ali, (2009), Effect of Impeller-Diffuser Radial Gap Ratio in Centrifugal Pump, Journal of Scientific & Industrial Research, Vol. 72, pp. 203-213.

[17] Spence R. and Amaral-Teixeira J., (2009), A CFD Parameter Study of Geometrical Variations on The Pressure Pulsations and Performance Characteristics of a Centrifugal Pump, Computers & Fluids, Vol. 38, pp. 1243-1257.

[18] Warman, (2009), Slurry Pump Handbook, Electronic Version, Fifth Edition, pp. 1-565.

[19] Yassine K. C., Hammoud A. H. and Khalil M.F., (2010), Experimental Investigation for Centrifugal Slurry Pump Performance, Tenth International congress of fluid Dynamics, pp. 1-9.

[20] Houlin Liu, Yong Wang, Shouqi Yuan, Minggao Tan and Kai Wang, (2010), Effects of Blade Number on Characteristics of Centrifugal Pumps, Chinese Journal of Mechanical Engineering, Vol. 23, pp. 1-6.

[21] Pagalthivarthi Krishnan V., Gupta Pankaj K., tyagi Vipin and Ravi M.R., (2011), CFD Predictions of Dense Slurrry flow in Centrifugal Pump Casings, International Journal of Aerospace and Mechanical Engineering, Vol. 5, pp. 254-266.

[22] Jafarzadeh B., Hajari A,. Alishahi M.M. and Akabri M.H., (2011), The Flow Simulation of a Low-Specific-Speed High-Speed Centrifugal Pump, Applied Mathematical Modelling, Vol. 35, pp. 242-249.

[23] Aman Abdulkadir, Kore Sileshi and Dribss, (2011), Flow Simulation and Performance Prediction of Centrifugal Pumps using CFD, Journal of EEA, Vol. 28, pp. 59-65.

[24] Yuan Jianping, Zhang Weijie, Jin Rong, Li Shujuan and Sunflow Wei, (2011), Flow Numerical Analysis within Auxiliary-Impellers of Centrifugal Pumps, International Conference on Information Science and Technology Nanjing, Jiangsu, China, pp. 1159-1163.

[25] Yang Sunsheng, Kong Fanyu and Chen Bin, (2011), Research on Pump Volute Design Method Using CFD, International Journal of Rotating machinery, Vol. 2011, pp. 1-7.

[26] Yi Li, Zuchao Zhu, Zhaohui He and Weiqiang He, (2011), Abrasion Characteristic Analysis of Solid-Liquid Two-Phase Centrifugal Pump, Journal of Thermal Science, Vol. 20, pp. 283-287.

[27] Datta Saikat, (2012), Numerical Investigation of Flow-Field inside a Centrifugal Slurry Pump Casing, M.tech thesis of Jadaypur University Kolkata, pp. 1-109.

[28] Yi Li, Zuchao Zhu, Weiqiang He and Zhaohui He, (2012), Numerical Simulation and Experimental Research on the Influence of Solid-Phase Characteristics on Centrifugal Pump Performance, Chinese Journal of mechanical Engineering, Vol. 25, pp. 184-189.

[29] Liu Y, Jiang Y and J Han Z, (2012), Research on the Pattern of Solid-Liquid two-Phase Distribution in Chemical process Pump, IOP Conference on Earth and Environmental Science 15, pp. 1-8.

[30] Shojaeefard M.H., Tahani M., Ehghaghi M.B., Fallahian M.A. and M. Beglari,(2012), Numerical Study of the Effects of Some Geometric Characteristics of a Centrifugal Pump Impeller That Pumps a Viscous Fluid, Computer and Fluid, Vol. 60, pp. 61-70.

[31] Ge X F, Gao Z X, Zheng Y and Shen M.H.,(2012), Efficiency calculation and the Vortex Characteristics Research of Centrifugal Pump, Earth and Environmental Science, Vol. 15, pp.1-6.

[32] Hedi Lamloumi, Hatem Kanfoudi and Ridha Zgolli, (2012), Simulation Study and Three-Dimensional Numerical Flow in a Centrifugal Pumps, International Journal of Thermal Technologies, Vol. 2, pp. 209-215.

[33] Wang P. W., Zhao J., Zou W.J. and Hu S.G., (2012), Experimental Study and Numerical Simulation of the Solid-Phase Particles Influence on Outside Characteristics of Slurry Pump, IOP Conference on Earth and Environmental Science 15, pp. 1-8.

[34] Jin Hyun Bae, Kim Myung Jin and Chung Wui Jun, (2012), A Study on the Effect of Variation of the Cross-sectional Area of Spiral Volute Casing for centrifugal Pump, World Academy of Science, Engineering and Technology Vol. 68, pp. 1897-1906.

[35] Zhao B. J., Huang Z. F., Chen H.L. and Hou D.H., (2012), Numerical Investigation of Solid-Liquid Two Phase Flow in a Non-Clogging Centrifugal Pump at Off-Design Conditions, IOP Conference on Earth and Environmental Science 15, pp. 1-9.

[36] Chakraborty Sujoy, Pandey K.M., Roy Bidesh, (2012), Numerical Analysis on Effects of Blade Number Variations on Performance of Centrifugal Pumps with Various Rotational Speeds, International Journal of Current Engineering and Technology, Vol. 2, pp. 143-152.

[37] Kumar S., Mohapatra S.K. and Gandhi B.K., (2013), Investigation on Centrifugal Slurry Pump Performance with Variation of Operating Speed, International Journal of Mechanical and Materials Engineering, Vol. 8, pp. 40-47.

[38] Chakraborty Sujoy, Choudhari Kishan, Dutta Prasenjit, Debbarma Bishop, (2013), Prediction of Centrifugal Pumps with Variations of Blade Number, Journal of Scientific and Industrial Research, Vol. 72, pp. 373-378.

[39] Yuliang Zhang, Yi Li, Baoling CUI, Zuchao Zhu and Huashu Dou, (2013), Numerical Simulation and Analysis of Solid-Liquid Two Phase Flow, Chinese Journal of Mechanical Engineering, Vol. 26, pp. 1-8.

[40] Zhou Ling, Shi Weidong and Wu Suqing, (2013), Performance Optimization in a Centrifugal Pump Impeller by Orthogonal Experiment and Numerical Simulation, Advances in Mechanical Engineering, Vol. 2013, pp. 1-7.

[41] Kaewnai Suthep, Wongwises Somchai, (2013), Analysis of Flow Through a Double-Acting Inmeller with a Straight Radial Blades using CFD, International Journal of Applied Research in Mechanical Engineering, Vol. 3, pp. 37-43.

[42] Carrier Nicolas La Roche, Ngoma Guyh Dituba and Ghie Walid, (2013), Numerical Investigation of a First Stage of a Multistage centrifugal Pump Impeller, Diffuser with Return Vanes and Casing, ISRN Mechanical Engineering, Vol. 2013, pp. 1-15.

[43] Ozturk Adnan, Aydin Kadir, Sahin Besir and Pinarbasi Ali, (2013), Effect of Impeller Diffuser Radial Gap Ratio in a Centrifugal Pump, Journal of Scientific and Industrial Research, Vol. 68, pp. 203-213.

[44] Hussein, Mohammed Ali Mahmood, (2013), Effect of Rotational Speed Variation on the Static Pressure in the Centrifugal Pump, Journal of Mechanical and Civil Engineering, Vol. 8, pp. 83-94.